RESEARCH ARTICLE

miRNA normalization enables joint analysis of several datasets to increase sensitivity and to reveal novel miRNAs differentially expressed in breast cancer

Shay Ben-Elazar[1,2]*, Miriam Ragle Aure[3,4]*, Kristin Jonsdottir[5,6], Suvi-Katri Leivonen[7], Vessela N. Kristensen[3,4,8,9], Emiel A. M. Janssen[5,6], Kristine Kleivi Sahlberg[3,10], Ole Christian Lingjærde[3,11], Zohar Yakhini[2,12]*

1 School of Computer Science, Tel-Aviv University, Tel-Aviv, Israel, **2** Department of Computer Science, Interdisciplinary Center, Herzliya, Israel, **3** Department of Cancer Genetics, Institute for Cancer Research, Oslo University Hospital, Oslo, Norway, **4** Department of Medical Genetics, Institute of Clinical Medicine, University of Oslo and Oslo University Hospital, Oslo, Norway, **5** Department of Pathology, Stavanger University Hospital, Stavanger, Norway, **6** Department of Chemistry, Bioscience and Environmental Engineering, University of Stavanger, Stavanger, Norway, **7** Helsinki University Hospital Comprehensive Cancer Centre and University of Helsinki, Helsinki, Finland, **8** Institute for Clinical Medicine, University of Oslo, Oslo, Norway, **9** Department of Clinical Molecular Biology and Laboratory Science (EpiGen), Division of Medicine, Akershus University Hospital, Lørenskog, Norway, **10** Department of Research, Vestre Viken Hospital Trust, Drammen, Norway, **11** Centre for Cancer Biomedicine, University of Oslo, Oslo, Norway, **12** Department of Computer Science, Technion–Israel Institute of Technology, Haifa, Israel

* shay.benel@gmail.com (SBE); Miriam.Ragle.Aure@rr-research.no (MRA); zohar.yakhini@gmail.com (ZY)

Citation: Ben-Elazar S, Aure MR, Jonsdottir K, Leivonen S-K, Kristensen VN, Janssen EAM, et al. (2021) miRNA normalization enables joint analysis of several datasets to increase sensitivity and to reveal novel miRNAs differentially expressed in breast cancer. PLoS Comput Biol 17(2): e1008608. https://doi.org/10.1371/journal.pcbi.1008608

Editor: Denis Thieffry, Ecole Normale Supérieure, FRANCE

Received: June 10, 2020

Accepted: December 6, 2020

Published: February 10, 2021

Peer Review History: PLOS recognizes the benefits of transparency in the peer review process; therefore, we enable the publication of all of the content of peer review and author responses alongside final, published articles. The editorial history of this article is available here: https://doi.org/10.1371/journal.pcbi.1008608

Data Availability Statement: All relevant data are within the manuscript and its Supporting Information files.

Abstract

Different miRNA profiling protocols and technologies introduce differences in the resulting quantitative expression profiles. These include differences in the presence (and measurability) of certain miRNAs. We present and examine a method based on quantile normalization, Adjusted Quantile Normalization (AQuN), to combine miRNA expression data from multiple studies in breast cancer into a single joint dataset for integrative analysis. By pooling multiple datasets, we obtain increased statistical power, surfacing patterns that do not emerge as statistically significant when separately analyzing these datasets. To merge several datasets, as we do here, one needs to overcome both technical and batch differences between these datasets. We compare several approaches for merging and jointly analyzing miRNA datasets. We investigate the statistical confidence for known results and highlight potential new findings that resulted from the joint analysis using AQuN. In particular, we detect several miRNAs to be differentially expressed in estrogen receptor (ER) positive versus ER negative samples. In addition, we identify new potential biomarkers and therapeutic targets for both clinical groups. As a specific example, using the AQuN-derived dataset we detect hsa-miR-193b-5p to have a statistically significant over-expression in the ER positive group, a phenomenon that was not previously reported. Furthermore, as demonstrated by functional assays in breast cancer cell lines, overexpression of hsa-miR-193b-5p in breast cancer cell lines resulted in decreased cell viability in addition to inducing apoptosis. Together, these observations suggest a novel functional role for this miRNA in breast cancer.

Funding: Helse Vest (https://helse-vest.no/en) grant 911450 was received by KJ. This project has received funding from the European Union's Horizon 2020 Research and Innovation Programme (https://ec.europa.eu/programmes/horizon2020/en) under Grant agreement No. 847912. The funders had no role in study design, data collection and analysis, decision to publish, or preparation of the manuscript.

Competing interests: The authors have declared that no competing interests exist.

Packages implementing AQuN are provided for Python and Matlab: https://github.com/YakhiniGroup/PyAQN.

Author summary

This work demonstrates a practical approach to the joint-analysis of multiple miRNA expression profiling datasets acquired with different measurement technologies. The use of different platforms in miRNA profiling can lead to major differences in results. In particular, some miRNA species are less amenable to detection and quantification by certain platforms or designs. Our approach, termed AQuN, combines quantile normalization with special attention to missing entities, to normalize miRNA expression across datasets, technologies, designs and platforms. As we show, our proposed approach uncovers patterns of interest that would not have emerged as statistically significant when analyzing the datasets individually or with other standard-practice normalization methods.

Amongst our findings, we noted a previously undocumented miRNA that is significantly over-expressed in samples from estrogen-receptor positive breast cancer patients as compared to samples from estrogen-receptor negative patients. We further investigated this miRNA, hsa-miR-193b-5p, and experimentally show, in cell lines, that its expression level impacts the viability of tumor cells. AQuN is available to the community in the form of Python and Matlab packages. The joint-processed data is also made available for further investigation.

Introduction

microRNAs (miRNAs) are endogenous, small non-coding RNAs (~22 nucleotides) that bind to target-specific sites most often found in the 3'-untranslated regions (UTRs) of target messenger RNAs (mRNAs). Through this binding, miRNAs regulate gene expression by conferring inhibition of mRNA translation or mRNA degradation [1]. miRNA expression profiling is an important tool for studying tumor biology and classification and serves as a basis for potential diagnostic and prognostic assessments [2–4]. Increasing technological and economic viability of expression sampling methods has enabled the systematic study of miRNA expression in cohorts of hundreds of patients [5–7] and in several cancer types [8, 9]. On the other hand, inherent measurement noise coupled with complex causes of biological variability affect the statistical confidence in ascertaining consistent differences of low magnitude between populations when limited to small sample sizes. Absolute expression differences are not necessarily linearly correlated with downstream effects of the expressed miRNA, therefore subtle but consistent differences may be of greater biological importance.

Abnormal miRNA expression in breast cancer has been repeatedly associated with cancer proteins [10], molecular subtypes [11], progression [12–14] and prognosis [5]. For example, in one of the first genome-wide characterization studies of miRNA expression in breast cancer we identified 63 miRNAs differentially expressed between the two main clinically diverse groups of breast cancer, estrogen receptor (ER) positive and the ER negative tumors [11].

Combining experimentally measured data from multiple sources is both a challenging and a worthwhile endeavor. Statistical estimation theory formulates a relation between sample size and variance of estimate via the Fisher information that follows the chain rule for independent samples. The ability of statistical hypothesis tests to detect subtle, yet consistent and possibly genuine, differences between populations is directly related to sample size and is quantified as a test's power [15, 16]. Increasingly larger power and statistical significance is hindered by sampling costs that can prohibit large sample sizes. This, in turn, leads to the incremental funding of repeated studies aiming to measure the same phenomenon. Follow-up studies tend to vary from their former, sometimes using newer or alternative experimental protocols, reagents and technologies, introducing batch differences between samples. Such a 'batching' design, inadvertently, introduces distinctions (batch effects) between samples that correlate with the batch and may overshadow subpopulation differences in their magnitude. Blindly testing for hypotheses on batch-collected dataset without taking such effects into account can lead to spurious and erroneous conclusions and can hide significant effects behind batch differences. In this work we address joint analysis of data batched using different miRNA profiling technologies that have been shown to have systematic differences [17, 18].

There are various approaches commonly used in practice to address the analysis of combined data containing batch effects. The authors of earlier works [19, 20] showed that applying standard, parametric, batch correction approaches may introduce bias from uneven sample sizes of the different groups and data idiosyncrasies. A recent study [21] applied a non-parametric approach for correcting case-control microbiome studies and showed that it compares favorably with former methods. Their method resembles ours, as we further illustrate below.

In this work we apply a non-parametric, quantile-based, batch normalization approach, Adjusted Quantile Normalization (AQuN). We use this method for jointly analyzing miRNA expression data in four breast cancer cohorts to obtain increased statistical confidence and power. We demonstrate that, coupled with appropriate non-parametric statistics, our normalization approach lowers the confounding impact of batch effects. We observe stronger statistical evidence of differential expression between ER positive and ER negative clinical groups in multiple miRNAs when compared to individually analyzing the cohorts. Moreover, our approach provides interpretable results and is advantageous to direct interpretation of the data, conducive to individual examination of findings, as demonstrated herein. Our differential expression analysis supports the use of AQuN by surfacing known cancer-related miRNAs, as well as providing evidence of potential new ones.

In particular, previous studies have showed hsa-miR-193b-3p regulates breast cancer migration [22] and can function as a metastatic suppressor [23]. Here we discovered that hsa-miR-193b-5p is significantly over-expressed in ER positive, compared to ER negative clinical groups. We propose that this difference is of functional significance and further show it leads to decreased cell viability and increased apoptosis.

Results

We apply the Adjusted Quantile Normalization (AQuN) process to the datasets described in [5, 11, 24–26] and illustrate the benefit and effects of this normalization step as related to data properties and to various downstream analysis steps in the subsections below.

AQuN is a novel variant of quantile normalization which utilizes quantization in its normalization process, thereby offering an added degree of control over noise that affects sample ranking and is evidently prevalent in miRNA datasets. Details of this method are available in the Materials and Methods section. Below we illustrate AQuN's advantage over standard normalization methods in uncovering, otherwise nascent, signals in the joint dataset.

Differential expression reveals novel breast-cancer associated miRNA

We performed a differential expression analysis comparing clinically relevant subgroups of breast cancer. We measured differential expression of a specific miRNA on a pair of sample

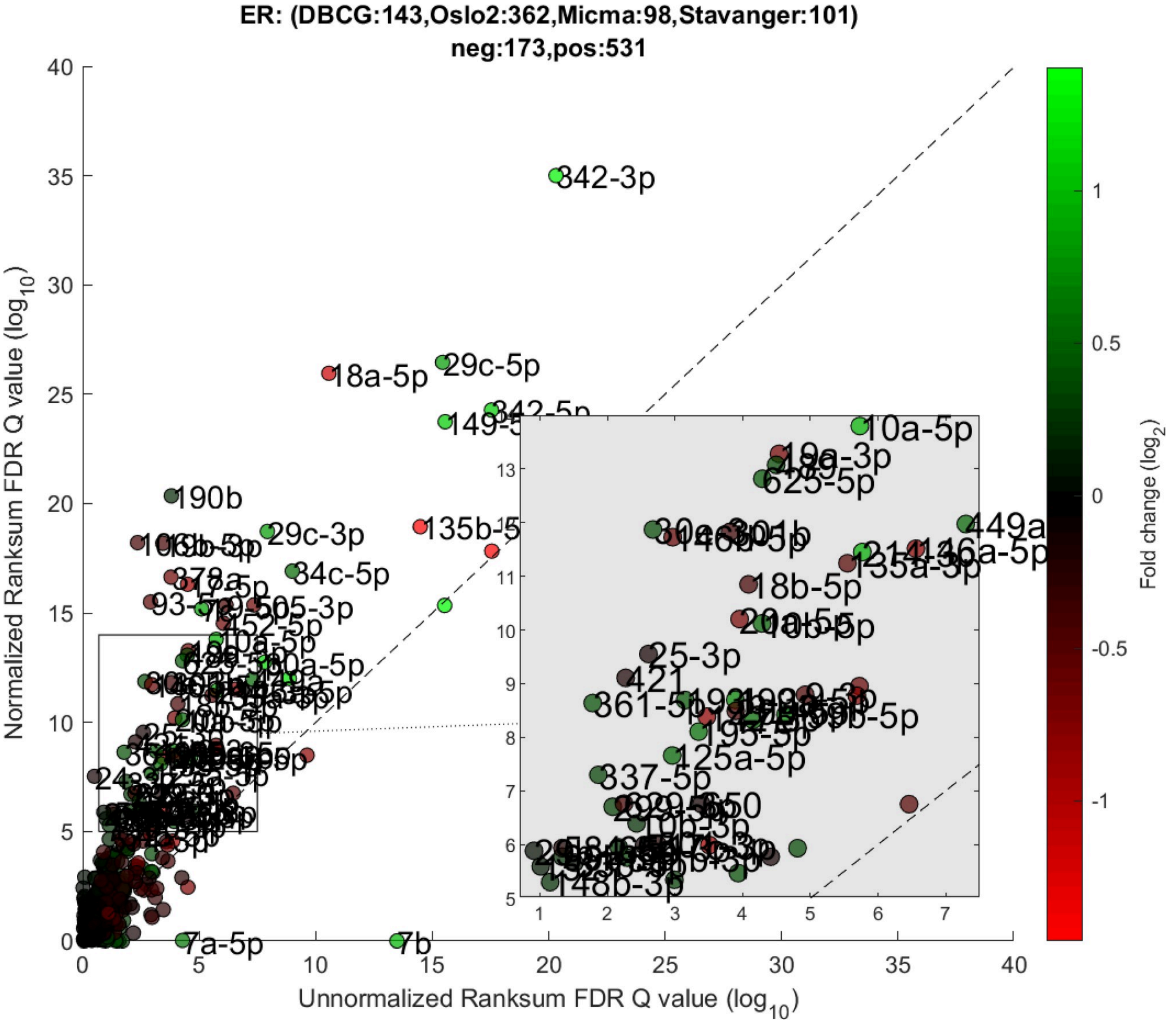

Fig 1. Differential miRNA expression between ER positive and negative. A scatter plot of differential expression p-values (-$\log_{10}$, Wilcoxon Rank-sum) for the unnormalized (x) vs normalized (y) joint dataset. Title contains sample size details and dataset distribution.

https://doi.org/10.1371/journal.pcbi.1008608.g001

subpopulations (e.g. ER positive vs ER negative). Fold-change was defined as the ratio ($\log_2$) between median expression of both sets. We applied Wilcoxon Rank-Sum (WRS) 1-tailed tests and resulting p-values were corrected across miRNAs using false discovery rates (FDR). Figs 1–3 showcases our differential expression analysis results for ER status. In Fig 1 scatter plot, we observe that the AQuN normalized dataset yields more significant results (lower Q-values) for most miRNAs (482/655). Fig 2 volcano plot illustrates that the increase in significance is not necessarily correlated with effect size (i.e. fold change), and that we gain confidence on lower effect sizes as anticipated by our power analysis (more details in the 4th paragraph of the Discussion section). In Fig 3 cumulative distribution function (CDF) plot we depict the overall trend of increased statistical significance, contrasted by even lower statistical significance that would be obtained from performing the differential expression analysis on each dataset separately (shown as dashed lines). In addition, we present the CDF plots that would be obtained

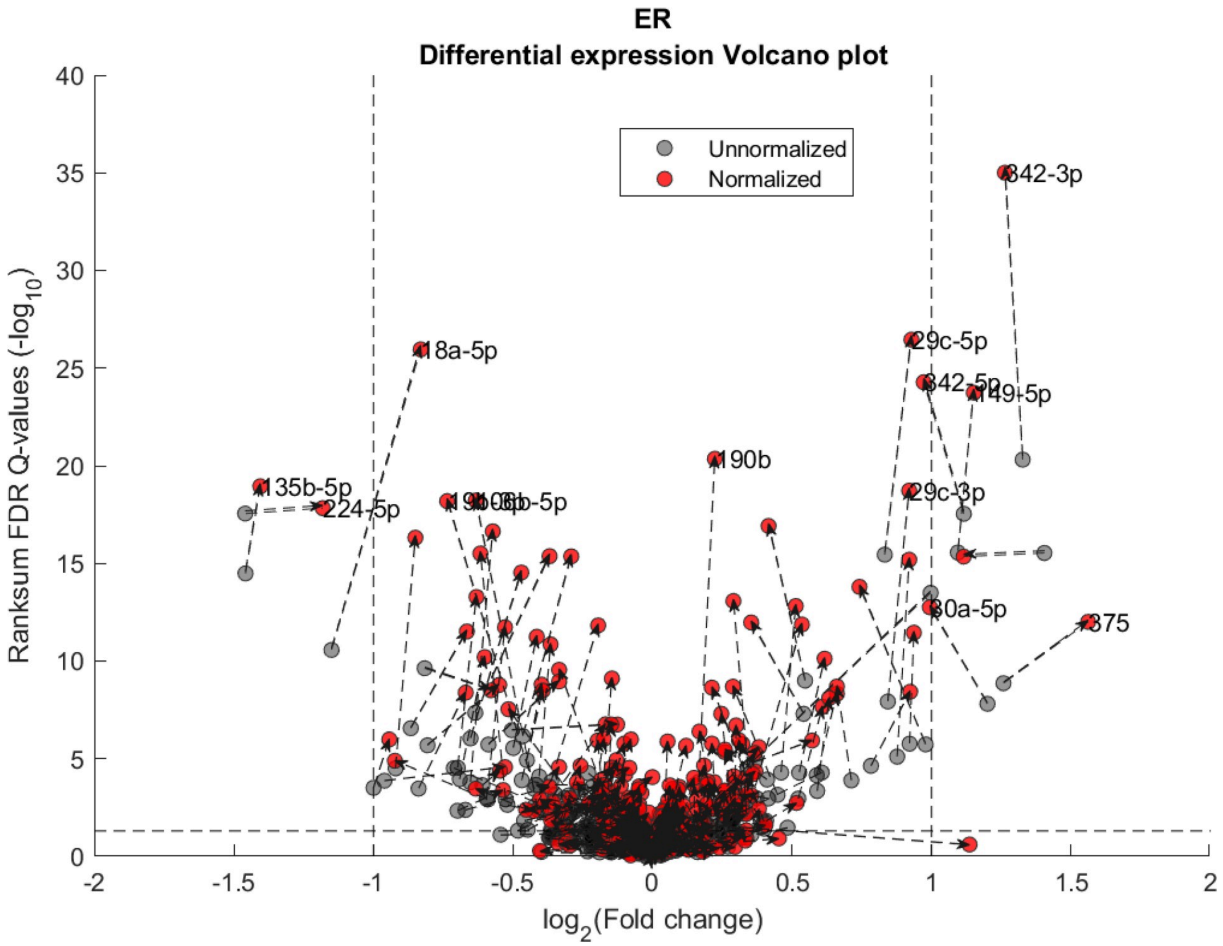

Fig 2. Differential miRNA expression between ER positive and negative. Volcano plot showing the fold change and corresponding Wilcoxon Rank-sum FDR corrected Q value ratio between the normalized and unnormalized datasets. Dashed arrow connects the unnormalized (gray circles) and normalized (red circles) results on a particular miRNA. High absolute values in X axis correspond to substantial difference in median expression between ER negative over ER positive samples (for a particular miRNA). High values in Y axis correspond to miRNAs that present substantial difference *after* normalization but not before. Low values in Y axis correspond to miRNAs that present substantial difference *before* normalization but not after. Vertical dashed lines represent a Fold change threshold of 2x ($\log_2(2)$ = 1) and horizontal dashed lines represent a Q-value threshold of 0.05 ($-\log_{10}(0.05) \cong 1.3$).

https://doi.org/10.1371/journal.pcbi.1008608.g002

by (individually) applying four commonly used normalization methods (shown as dotted lines). Evaluated normalization methods include:

- Mean ratio: scales each sample by $M(i,j) = \frac{M(i,j)}{Avg\ M(:,j)}$.
- Median subtraction: subtracts the median of each sample, then sets the minimum of each sample to the (global) minimum across samples. I.e.:

$M(i,j) = M(i,j) - Medial\ M(:,j)$. min $M(:,j) \leftarrow$ min $M(:,:)$

- Vanilla quantile: MATLAB's implementation of Quantile Normalization also known as Quantile Standardization [27].
- ComBat [28]: empirical Bayes batch effect mitigation employing a design matrix that includes dataset batching along with clinical labels and status of Tumor grade, Subtype, ER, PR, HER2 and TP53. We apply the QR decomposition [29] to mitigate any co-linearity in the design matrix.

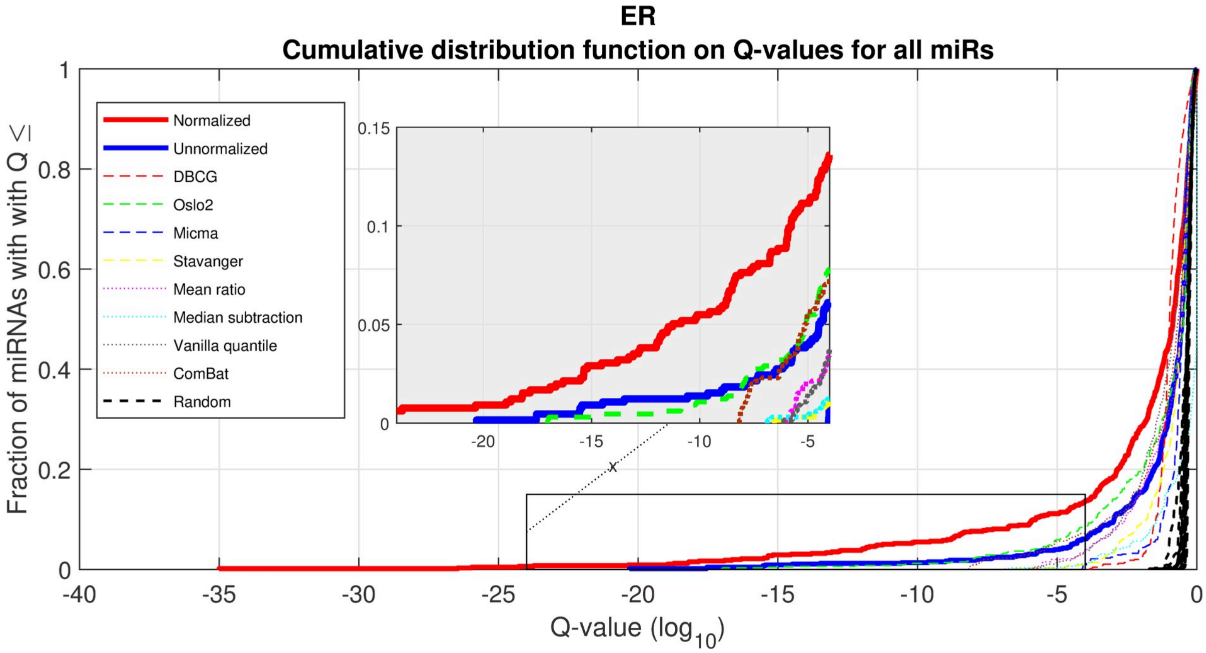

Fig 3. Differential miRNA expression between ER positive and negative. A CDF plot showing many more substantially differentially expressed miRNAs after normalization (red line) than before normalization (blue line), and substantially more than would be expected at random (compared to 20 random permutations of labels, dashed black lines). Also shown are dashed colored lines corresponding to each appropriate single-dataset Q values exemplifying the advantage of a joint-dataset analysis. Note that at Q = 10^{-18} we can find 10 miRNAs under AQuN but none under other normalization approaches or per dataset analyses.

https://doi.org/10.1371/journal.pcbi.1008608.g003

In Figs 4 and 5 we demonstrate the impact of normalization on single miRNAs (hsa-miR-190b and hsa-miR-18a-5p, accordingly) across samples and on their differential expression in the context of ER status. This is done by detailing expression values for each sample in the joint dataset prior to (top row) and following (bottom row) AQuN normalization. We present the medians of each clinical group (dashed horizontal lines) and a breakdown of how samples of both clinical groups are distributed when sorted by value and when compared to a uniform null model. This provides a qualitative view of the effect normalization has on both individual samples and datasets in the context of the investigated differential expression. Previous studies [30] have shown hsa-miR-190b to be linked to ER status and further suggested its use as a potential biomarker. Similarly, hsa-miR-18a-5p is an oncogene and prognostic biomarker [31]. As we have shown in the volcano plot in Fig 2, hsa-miR-190b would not have been identified as differentially expressed in ER positive vs negative samples prior to normalization. Similar plots for the top 40 differentially expressed miRNA (post-normalization) are available compressed in S1 Data.

When inspecting the differential expression results of all normalization methods, the unnormalized data and each dataset separately, there are 33 unique miRNAs that are only shown as significantly ($Q\ value<0.05$) differentially expressed in ER positive vs ER negative as identified by our normalization method (S2 Fig, S2 Text, list in S6 Table). Contrastingly, other approaches yield far fewer significantly differentially expressed miRNAs. Of the 33 miRNAs uniquely detected by our method, we present four in Table 1 that have fold change greater than 0.15 (absolute $\log_2 > 0.15$, which translates to $>$ 10% change between median expression of ER positive and ER negative tumors).

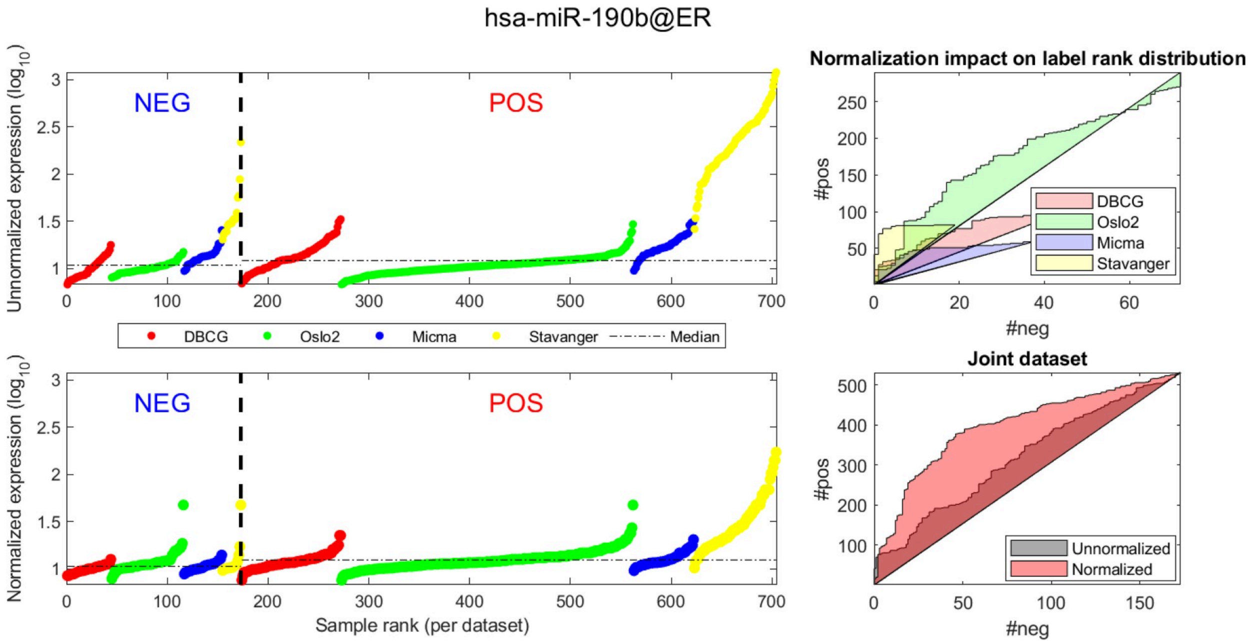

Fig 4. Visualizing expression of hsa-miR-190b across datasets and samples and in regard to estrogen receptor (ER) positive (pos) vs. negative (neg) differential expression. (A, D) Expression values ($\log_2$) of each sample before quantile normalization. Samples are ranked by ER status label, then by dataset and finally by ascending expression value. (A, B)-Unnormalized joint dataset. (C, D)-Normalized joint dataset. (B, C) Actual vs expected (via a uniform null model) rank distribution of ER negative (neg) vs positive (pos). Diagonal straight lines bounding a polygon represent a null uniform distribution of positive and negative samples (when ranked by expression value). The colored surface area represents the magnitude of deviation from a uniform distribution. The boundary of the surface is calculated by the cumulative number of ER negative (x axis) vs ER positive (y axis) samples in the ranked (descending) expression vector. Top-illustrating the rank distribution per-dataset (without normalization). Bottom-comparing the joint-dataset distributions when ranking before or after normalization.

https://doi.org/10.1371/journal.pcbi.1008608.g004

To study any breast cancer related functional significance of these top differentially expressed miRNAs we performed miRNA gain-of-function studies in the MCF-7 breast cancer cell line. Here, cell viability was measured as an endpoint after overexpression of the miRNAs. Indeed, one of the miRNAs, hsa-miR-193b-5p, showed a significant reduction in cell viability compared to miRNA negative controls (Fig 6). Furthermore, we looked into data from another functional experiment previously published [32] in the HER2 positive breast cancer cell line KPL4 and here we found that hsa-miR-193b-5p induced apoptosis (as measured by the levels of cleaved PARP), and downregulated the levels of HER2 and phosphorylated ERK upon overexpression. Altogether, these results suggest that miR-193b-5p may exert a tumor-suppressor function in breast cancer, both in an ER+ and a HER2+ context. Interestingly, the other miRNA originating from the same precursor, hsa-miR-193b-3p has been previously shown to directly target ESR1 mRNA and is thus a direct regulator of the ER [33].

Further investigation of the three other top differentially expressed miRNAs shows prior evidence linking them to cancer. For example, hsa-miR-601 is a known prognostic marker and potential tumor-suppressor in breast cancer [34] and hsa-miR-936 was identified as a potential tumor-suppressor miRNA in ovarian cancer [35]. While these findings do not directly validate our findings in ER differential expression, they support the potential association of these miRNA through related mechanisms of cancer pathogenesis.

Joint analysis with mRNA data

A similar pipeline to the one described in subsection “Dataset pre-processing and coverage” was used to parse the Oslo2 cohort mRNA expression data, using Limma.

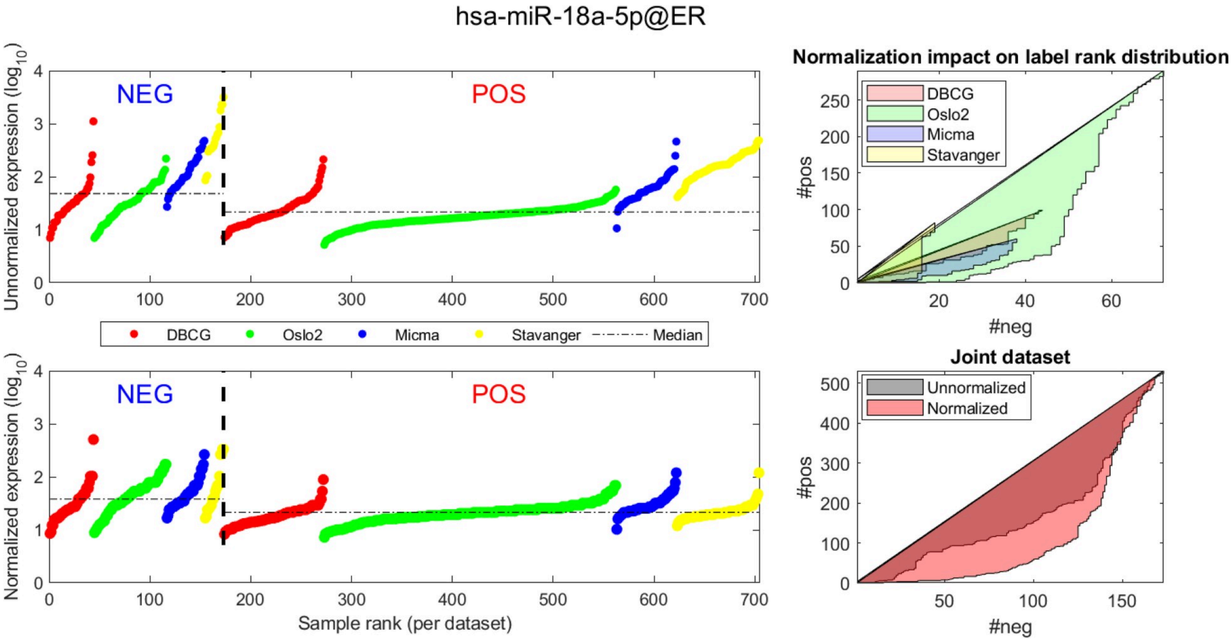

Fig 5. Visualizing expression of hsa-miR-18a across datasets and samples and in regard to estrogen receptor (ER) positive (pos) vs. negative (neg) differential expression. Caption description matches the one provided in Fig 4.

https://doi.org/10.1371/journal.pcbi.1008608.g005

We wanted to assess the effect of AQuN normalization on the results of enrichment analysis as performed using both mRNA and miRNA data. To this end we first formed a ranked list of transcripts as follows. For each miRNA, μ, we ranked all mRNAs according to the (ascending) Spearman correlation between the miRNA expression pattern across the entire dataset and the mRNA expression pattern across the entire dataset (paired on matching samples). We denote the resulting ranked gene list, with μ as a pivot, as $\mathcal{G}_\mu$.

Effect on gene target enrichment. For the first analysis we investigated the impact of AQuN normalization on correlations between miRNA and the expression levels of their expected mRNA targets in the Oslo2 dataset. We expect stronger negative correlation after normalization to direct gene targets. To validate this hypothesis, we applied a non-parametric, rank-based analysis using the MiTEA [36, 37] approach. MiTEA is used to evaluate the statistical association between $\mathcal{G}_\mu$ and $\mathcal{C}_\nu$, where $\mathcal{C}_\nu$ is a ranked list of genes wherein the ranking is based on the affinity of the gene as a target candidate for the miRNA ν, taken from TargetScan [38]. A short overview of MiTEA's algorithm is available in the Materials and Methods section.

We declare a matching if MiTEA returns a significant ($\leq$0.001) P-value when $\nu = \mu$. To recapitulate, a matching occurs if the top of two lists of genes overlap to a high degree: the

Table 1. Top differentially expressed miRNA sorted by fold change.

miRNA	Fold Change ($\log_2$)	Q-value
hsa-miR-601	-0.18	0.048
hsa-miR-424-3p	-0.17	0.0003
hsa-miR-936	-0.15	0.027
hsa-miR-193b-5p	0.19	0.0002

We apply AQuN normalization on the joint dataset and not detected by other approaches. Fold change is defined as $\log_2 \frac{Median\ ER\ positive}{Median\ ER\ negative}$.

https://doi.org/10.1371/journal.pcbi.1008608.t001

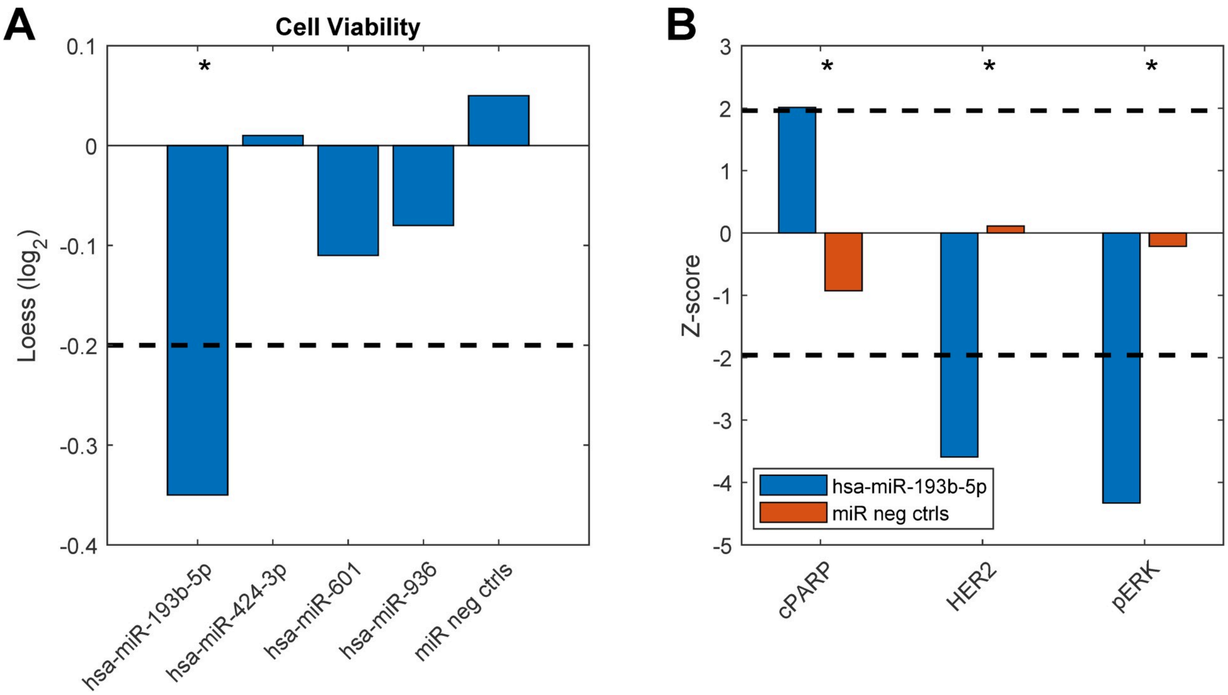

Fig 6. Functional experiment results. Breast cancer cell lines were transfected with miRNA mimics (20nM) and assayed for functional effects 72 hours after transfection. A) Cell viability measured in MCF7 breast cancer cells. B) Apoptosis measured by levels of cleaved PARP (cPARP), HER2 and phosphorylated ERK (pERK) protein levels measured in KPL4 cells. The dashed lines indicate cut-off points that were considered significant (see Materials and Methods). Asterisks denote significant effects. Original data from b) are taken from [32].

https://doi.org/10.1371/journal.pcbi.1008608.g006

prominent predicted gene targets (by TargetScan) of miRNA μ and the list of genes ranked according to their sample-wise anti-correlation with their matched expression levels of miRNA μ. When applying this procedure on a non-normalized miRNA expression we find no matchings. When applying the same procedure on AQuN normalized data we find 6 matchings as detailed in Table 2. For each matched miRNA we also provide supporting evidence of several studies describing its role in breast cancer. We included an extension of this analysis across other datasets and normalization approaches in S2 Table.

We show one such analysis in detail for *hsa-miR-29b* in Figs 7 and 8. Here we follow MiTEA's approach to obtain a statistical assessment of target enrichment for $\mu = \nu =$ *hsa-miR-*

Table 2. Resulting MiTEA matchings on normalized miRNA expression.

miRNA	P-value	Q-value	Corroborating studies
hsa-miR-29b	1.28E-08	1.73E-06	[39–41]
hsa-miR-106b	1.96E-06	1.11E-04	[42–44]
hsa-miR-200b	1.06E-04	5.54E-03	[45–47]
hsa-miR-30d	4.38E-04	1.19E-02	[48, 49]
hsa-miR-96	9.02E-05	1.53E-02	[50, 51]
hsa-miR-182	4.58E-04	4.43E-02	[52, 53]

P and Q values are color coded by magnitude where from green (more significant results) to red (less significant results). None of these statistically significant associations between pivot miRNAs and their targets is observed when using the raw, un-normalized data. Nor is any other matching miRNA target enrichment observed in the unnormalized data.

https://doi.org/10.1371/journal.pcbi.1008608.t002

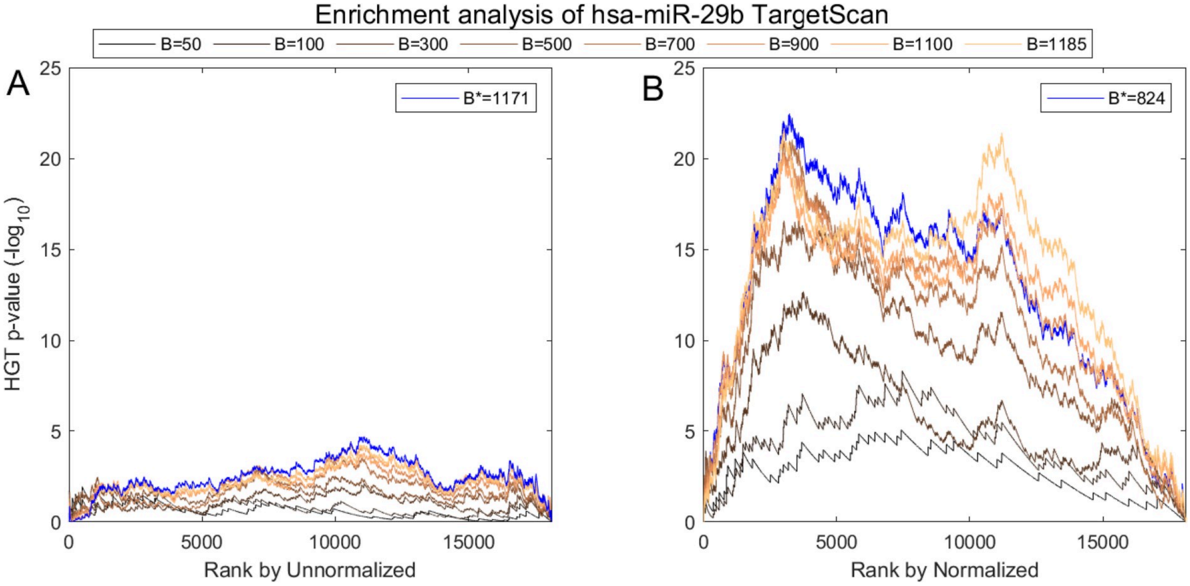

Fig 7. Impact of normalization on the correlation between hsa-miR-29b expression and its in-silico predicted targets according to TargetScan. (A) AQuN normalized vs Unnormalized (B) miRNA showing normalized is more negatively correlated to the prominent hsa-miR-29b targets in TargetScan as evident in stronger enrichment values.

https://doi.org/10.1371/journal.pcbi.1008608.g007

29b and $B = \{1, \ldots, |\mathcal{C}_v|\}$ binary vectors $\mathcal{B}(\mu, v, B)$. We present the results on various Bs and the optimal B^* for both unnormalized and normalized miRNA expression.

Effect on gene ontology (GO) enrichment. We applied GOrilla [36] to identify gene ontology enrichment in $\mathcal{G}_\mu$ on both unnormalized miRNA expression and on normalized miRNA expression. Given a ranked list $\mathcal{G}_\mu$, GOrilla produces a binary vector $\mathcal{B}(\mathcal{G}_\mu, \omega)$ for each gene ontology term, ω, in which a gene is labeled as binary '1' if it belongs to ω. Next, GOrilla computes mHG p-values, correcting them across GO terms. Fig 9 is a scatterplot comparing between our results on unnormalized and normalized hsa-miR-29b lists. The findings from this analysis are in line with previous studies that have linked the miR-29 family with tumor growth and metastasis [40, 54, 55].

Discussion

We have presented an integrative analysis technique and applied it to jointly analyze human breast cancer miRNA expression datasets spanning different studies and utilizing different measurement technologies. Our approach is powerful in its ability to increase statistical power without apparent adverse effects on precision, as exemplified by several downstream analysis results. Our normalization method (AQuN) is based on a slight adaptation to standard (a.k.a. vanilla) quantile normalization. Vanilla quantile normalization averages values across samples with the same rank, while our method averages values across samples within the same percentiles (computed per sample). This has the effect of lowering the impact of within-quantile noise when computing rank-based statistics. Additionally, our method, as defined, can support normalization of multiple cohorts that contain only partial overlaps in their evaluated miRNAs. Correctly applying AQuN requires a basic understanding of the impact it has on downstream statistics. In this work we focused on applying nonparametric rank-based statistics to downstream analyses. Our normalization approach can apply to parametric analyses as well. Further discussing parametric analysis is out of scope for this work. We offer a short discussion

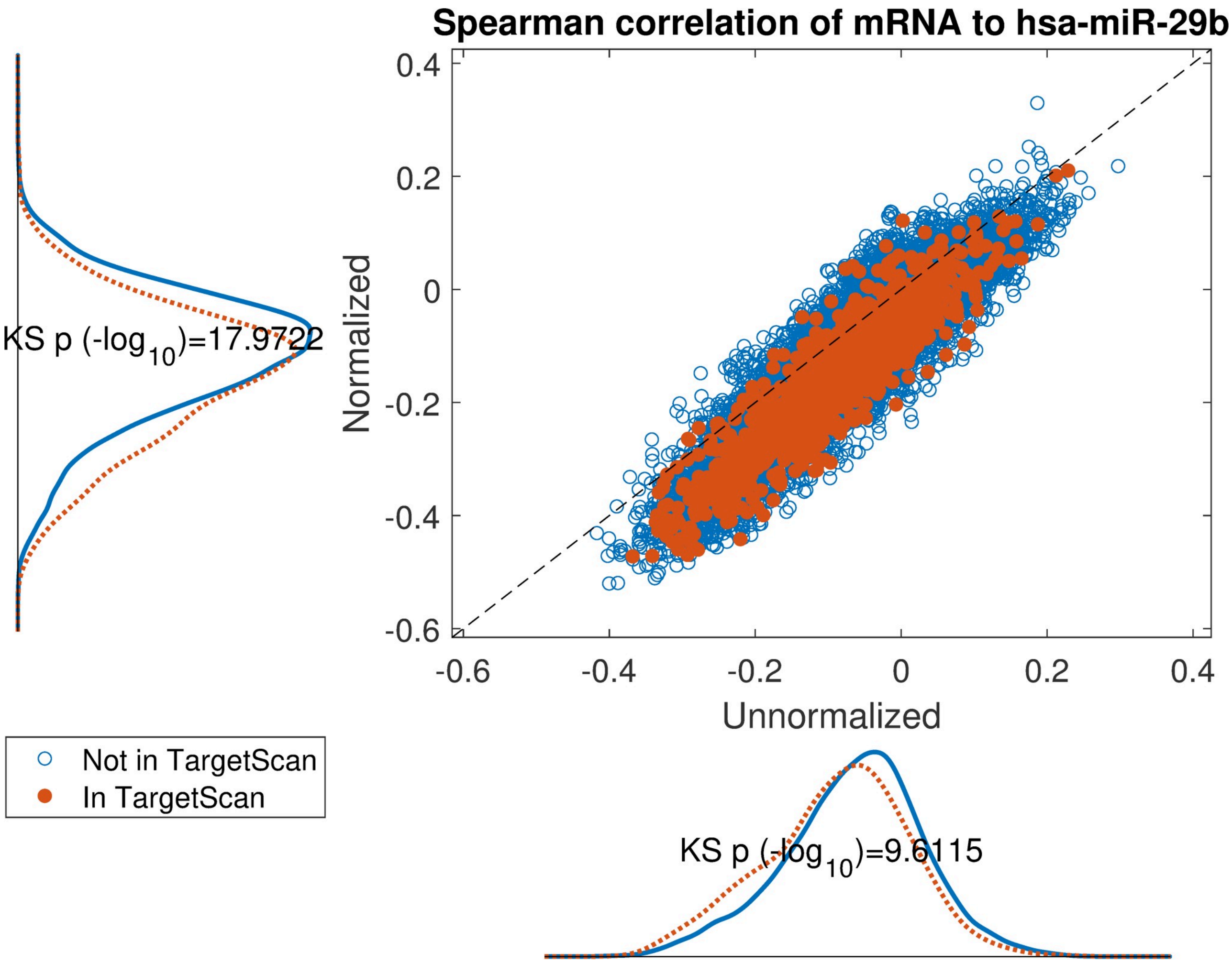

Fig 8. Impact of normalization on the correlation between hsa-miR-29b expression and its in-silico predicted targets according to TargetScan. Scatter plot of spearman correlation on normalized miRNA or unnormalized miRNA expression. If the target mRNA appears in TargetScan it is highlighted in orange. The marginal distributions are shown parallel to the axes and corresponding Kolmogorov-Smirnov test p-values display an overall lowered correlation for TargetScan candidates on normalized data.

https://doi.org/10.1371/journal.pcbi.1008608.g008

on the impact of normalization on intra-sample rankings and intra-miRNA rankings (see S3 Text and S3 Fig).

The first point to address, in terms of impact on downstream statistics is in the context of differential expression. We focus the discussion on ER related differential expression. When comparing the normalized joint dataset with per-dataset analyses we observe stronger p-values, yielding more statistically significant candidates after applying multiple hypothesis correction procedures. In Fig 3, we illustrate this result through a shift in the cumulative distribution of Wilcoxon Rank-sum FDR corrected Q-values calculated for the differential expression of ER positive and negative samples. In Fig 10 we present a per dataset drill-down in to the analysis presented in Fig 2. For some miRNAs, we observe a tradeoff between higher absolute fold-change and higher rank-sum -log$_{10}$ Q-values. For example note hsa-miR-135b that has >−8× fold change for Stavanger, but at a fairly low -log$_{10}$ Q-value < 4 while after joint analysis it demonstrates only >−2× fold change but at -log$_{10}$ Q-value > 18.

A second important point is the increase in statistical power that is afforded through the integration of several datasets. One of the main motivating reasons for jointly analyzing

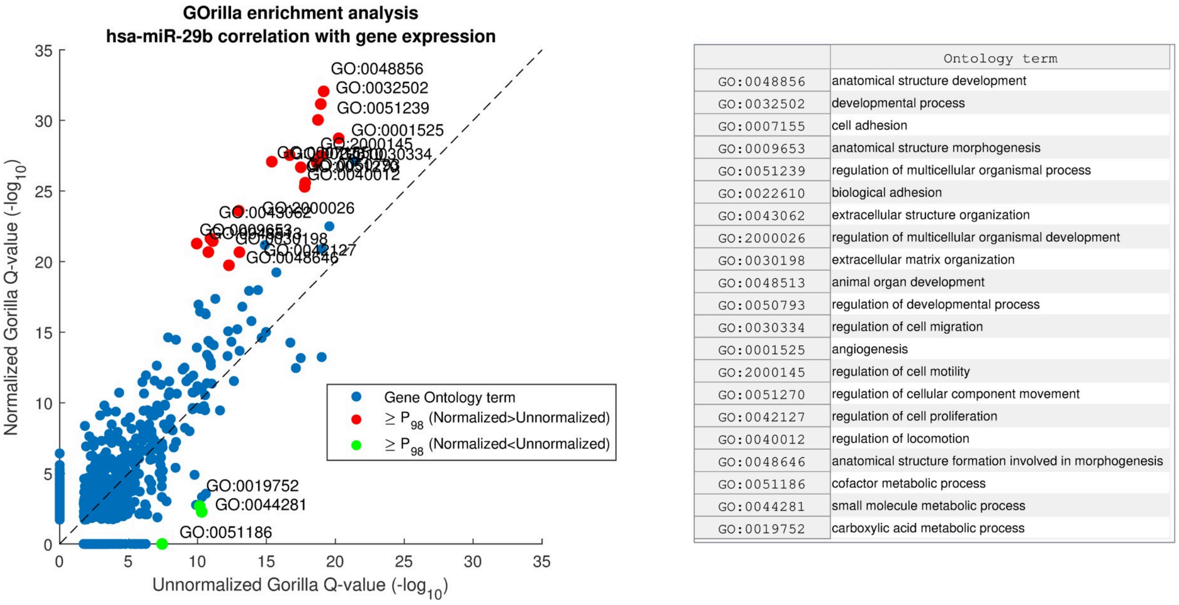

	Ontology term
GO:0048856	anatomical structure development
GO:0032502	developmental process
GO:0007155	cell adhesion
GO:0009653	anatomical structure morphogenesis
GO:0051239	regulation of multicellular organismal process
GO:0022610	biological adhesion
GO:0043062	extracellular structure organization
GO:2000026	regulation of multicellular organismal development
GO:0030198	extracellular matrix organization
GO:0048513	animal organ development
GO:0050793	regulation of developmental process
GO:0030334	regulation of cell migration
GO:0001525	angiogenesis
GO:2000145	regulation of cell motility
GO:0051270	regulation of cellular component movement
GO:0042127	regulation of cell proliferation
GO:0040012	regulation of locomotion
GO:0048646	anatomical structure formation involved in morphogenesis
GO:0051186	cofactor metabolic process
GO:0044281	small molecule metabolic process
GO:0019752	carboxylic acid metabolic process

Fig 9. GOrilla enrichment analysis comparison of hsa-miR-29b correlation with gene expression before and after miRNA normalization with AQuN. Showing scatter of GO term Q-values before and after AQuN. Red dots depicted with "≥P98" are above the 98th percentile of Normalized–Unnormalized Q-values (-$\log_{10}$) and green dots are for Unnormalized–Normalized. Right side panel shows a list of GO terms in the ≥P98 group.

https://doi.org/10.1371/journal.pcbi.1008608.g009

datasets collected in different places, times and possibly using different measurement technologies is the fact that the combined dataset supports higher statistical power. As we have shown in Fig 3, this increase of power is not attainable when naively joining the dataset or when normalizing with the presented alternatives.

We present a theoretical statistical a-priori power analysis [56] to put in context the advantage of jointly analyzing the datasets investigated in the current work. Remember that power is used in statistics to quantify the recall of a statistical test, i.e. the probability of correctly rejecting the null hypothesis. The test evaluated in this analysis is Wilcoxon rank-sum as applied for our differential expression analysis in the results section under subsection "Differential expression reveals novel breast-cancer associated miRNA". Power is only meaningful in the context of an expected effect size (measured herein using Cohen's d [57]), as larger differences and less variance in samples implies a smaller sample size is required to decide there is a difference between two populations. For the purpose of this analysis we assume allocation ratio = 1 (i.e. equal group sizes), while in the ER examples shown in Fig 11 actual ratios of Negative vs Positive ER samples are 0.44, 0.24, 0.63 0.23 and 0.32 for DBCG, Oslo2, Micma, Stavanger and Joint, accordingly–further reducing expected power. We overlay the theoretical plot with empirical effect sizes measured per dataset in hsa-miR-29b-3p and has-miR-18a-5p which we have identified as miRNAs of interest in Table 2 and Figs 4 and 5, accordingly.

A potential line of inquiry to follow up on from this study is to compare AQuN results on other sets of cohorts and with other normalization approaches. We have applied a preliminary analysis on a second set of cohorts, consisting of the TCGA [58] and Tahiri [14] cohorts. We performed a differential expression analysis comparing cancer and control samples and include a 5th normalization method previously referenced which is relevant in the context of case-vs-control experimental setups. Our results are presented in S4 Fig. When sorting miRNA according to their differential expression -$\log_{10}$(Q-value), we observe many known oncomiRs [59] are ranked higher and have more significant Q-values (S1 Table).

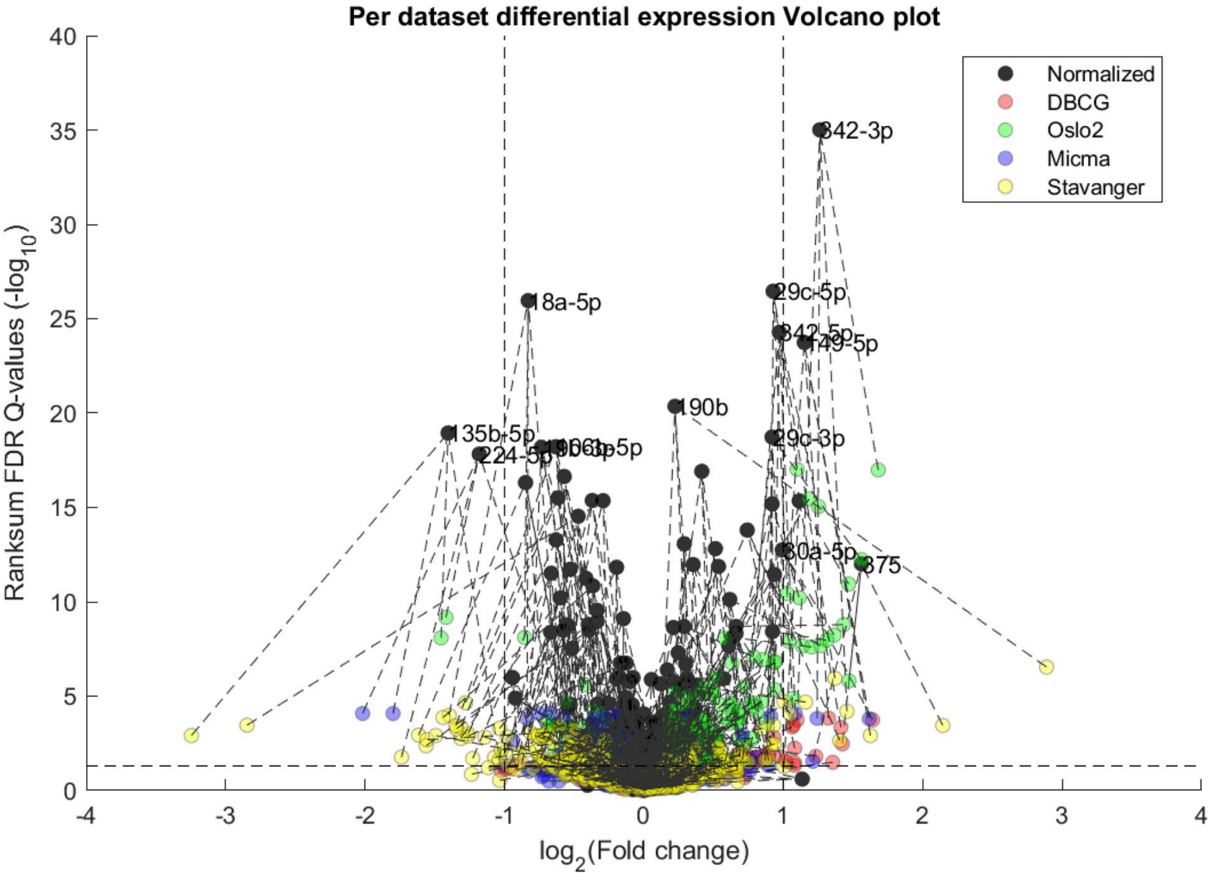

Fig 10. Volcano plot of per-dataset Differential Expression of ER positive vs ER negative from Fig 1. Here we include a both joint normalized and per dataset results. We observe an overall increase in statistical significance as dark points tend to be higher on the y-axis than their corresponding-colored points (indicated by dashed lines), as would be expected from the increase in statistical power. In some miRNA this can come at the cost of a lower detected fold-change as compared to some individual datasets.

https://doi.org/10.1371/journal.pcbi.1008608.g010

Overall, we provide multiple lines of evidence supporting the joint analysis of miRNA expression using nonparametric statistics. Our analysis yields potential novel biomarkers as exemplified by hsa-miR-193b-5p and its potential tumor-suppressor role in breast cancer. While these results require further validation, we demonstrate how stronger statistical evidence can be obtained in suggesting candidates and in prioritizing follow-up studies.

Materials and methods

Ethics statement

The Stavanger cohort was approved by REC Region West, approval number 2010/2014. By this approval, none of the patients were required to provide written informed consent to participate. All insights in a patient's journal were monitored electronically, and all except the treating physician were required to state the reason why they needed to read that patient's journal. This log was always open for the patient to view.

Overview

We used miRNA expression data from three previously published breast cancer datasets along with a newly released, fourth, miRNA dataset. These datasets were acquired from fresh-frozen

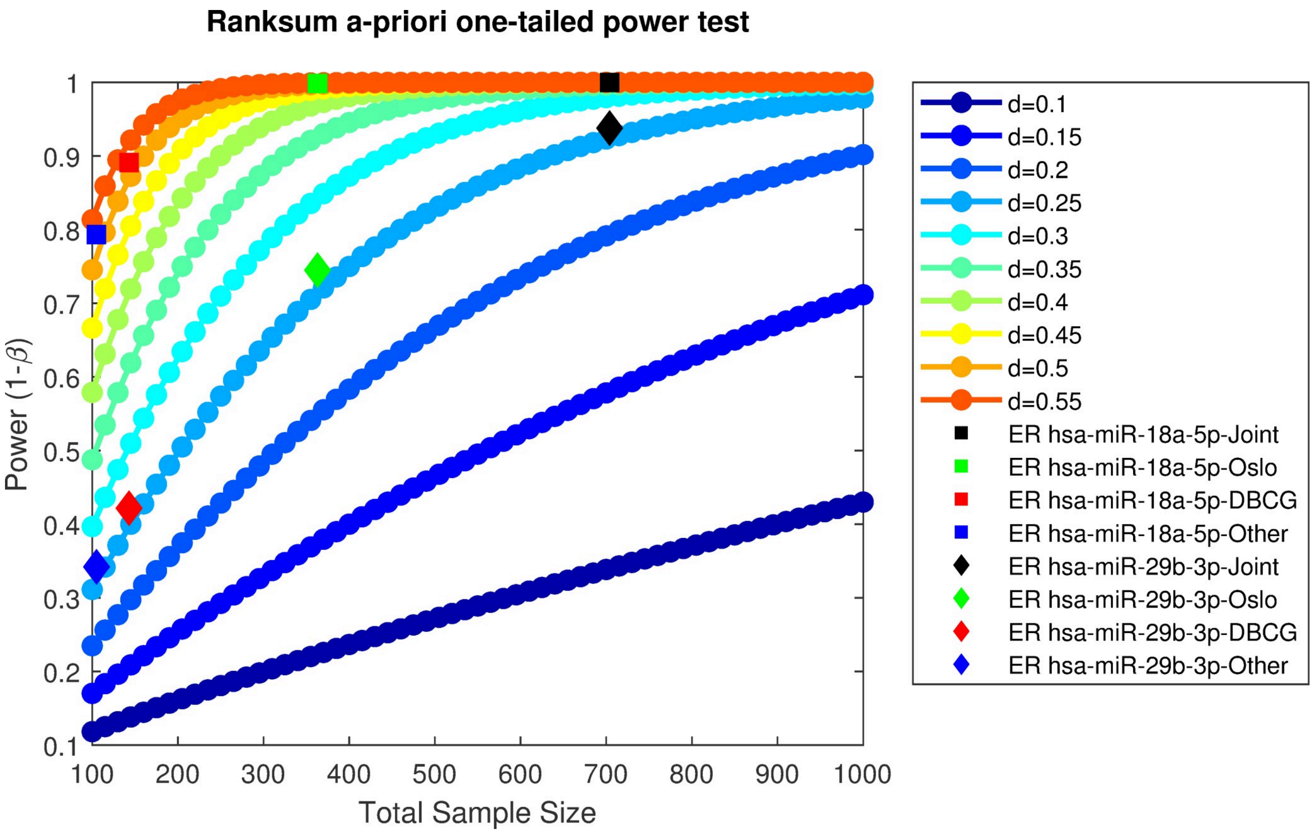

Fig 11. Statistical power as a function of sample size and expected effect size (measured in Cohen's d [66]). Dotted line plots illustrate an a-priori power analysis for one-tailed Wilcoxon Rank Sum (WRS) test for different effect sizes. Overlaid in squares and triangles are effect sizes, d, for the differential expression of hsa-miR-18a-5p and hsa-miR-29b-3p, accordingly, in ER positive vs ER negative samples as estimated empirically over the joint dataset on non-normalized data. Power values are estimated via (linear, 2D) interpolation on different dataset sizes.

https://doi.org/10.1371/journal.pcbi.1008608.g011

material with different minimal number of tumor cells criteria, using different technologies and experimental protocols as overviewed in Table 3. In addition, we utilized mRNA expression to further investigate the effect of normalization using one of the cohorts. We examine miRNA normalization also in the context of jointly analyzing these measurements. Below we elaborate our considerations in the selections made during the normalization process and our means of providing evidence for validating these results.

Table 3. Technical details of platforms used for expression measurements for the four different cohorts.

Color code	Dataset	Manufacturer	Technology	Version	Accession number	Number of samples
🟫	**DBCG[25]–miRNA**	**Agilent**	**Human miRNA Microarray Kit**	**(V2 G4470B) design id 019118**	**GSE46934**	**149**
🟩	**Oslo2[15]–miRNA**	**Agilent**	**Human miRNA Microarray Kit (V2)**	**v14 Rev.2 design id 029297**	**GSE81000**	**425**
🟩	**Oslo2[15]–mRNA**	**Agilent**	**SurePrint G3 Human GE 8x60K Microarray**	**(Probe Name Version) 028004**	**GSE80999**	**381**
🟦	**Micma[11]–miRNA**	**Agilent**	**Human miRNA Microarray Kit**	**(V2 G4470B) design id 019118**	**GSE19536**	**101**
🟨	**Stavanger–miRNA**	**Exiqon**	**miRCURY LNA Array**	**v.11.0**		**109**

Datasets are color coded consistently throughout the paper. miRNA expression colors are highlighted compared to mRNA measurements.

https://doi.org/10.1371/journal.pcbi.1008608.t003

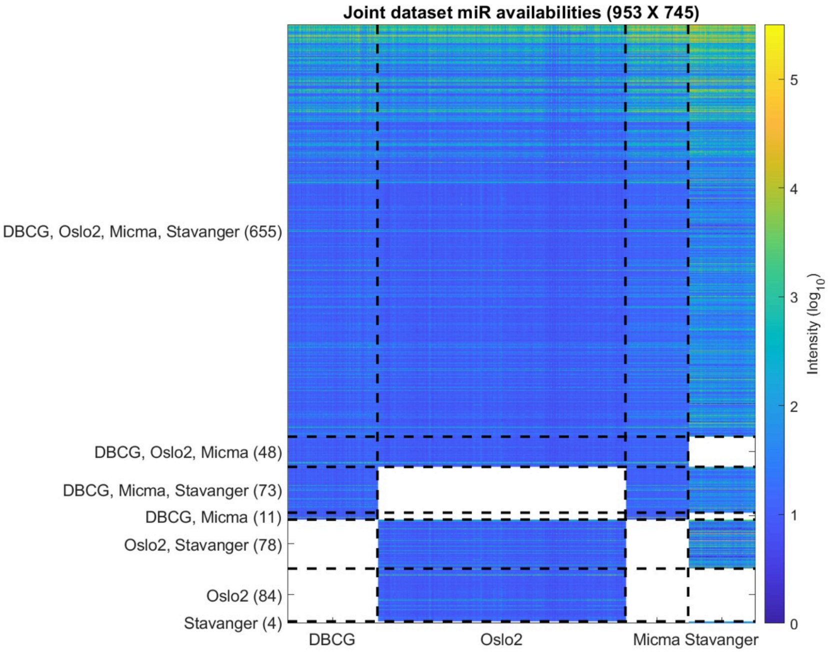

Fig 12. Overview of the miRNA coverage in the dataset. Each row represents one miRNA. Each entry represents the intensity ($\log_{10}$) in a specific sample. Dashed vertical lines separate between samples from the four datasets. Dashed horizontal lines separate between groups of miRNAs by their dataset availability. Blank (white) entries correspond to miRNAs that are missing from a dataset.

https://doi.org/10.1371/journal.pcbi.1008608.g012

Dataset pre-processing and coverage

Each miRNA dataset is read from a single-channel image analysis output file acquired from their corresponding GEO repositories (referenced in Table 3) and preprocessed in R using the Limma [60] package. We note that while Stavanger (Exiqon) data contains a pooled-reference second channel, this measurement is not utilized in our analysis (further discussed in S1 Text). Initially, control probes are removed, and the data is corrected by background intensity normalization [61]. Same-probe replicate samples are replaced by their median value. Probe ids are mapped to their corresponding miRbase v22 accession using miRBaseConverter [62]. Missing or deleted accession IDs are discarded. Multiple probes that map to the same miRNAs are again replaced by their median value. Next, we apply arrayQualityMetrics [63] (resulting Quality Control reports are available compressed in S2 and S3 Data) and filter out samples that are marked as outliers by all three outlier detection criteria (L_1-Distance between arrays, Boxplot, MA plot). We thereby filtered out 6, 30, 12 and 2 outliers from DBCG, Oslo2, Micma and Stavanger, respectively. Next, we apply minimum subtraction to avoid log scaling issues with negative numbers where applicable. The joint dataset table is then compiled by applying a "full outer-join" relational operation on the miRbase accession IDs as key. The resulting miRNA cross-dataset table is visualized in Fig 12 (and available in S3 Table as raw data and S4 Table as normalized data with corresponding clinical labels in S5 Table).

Batch effects in joint data. We tested for rank-order consistency of miRNA expression in pairs of datasets (Fig 13). For each miRNA we take the median of its expression, or similarly, intra-sample percentile, across all samples belonging to the same dataset. We display the resulting values for each pair of datasets in a scatterplot matrix considering the miRNAs (n = 655) present in all four cohorts. This analysis shows that the Stavanger data appears to

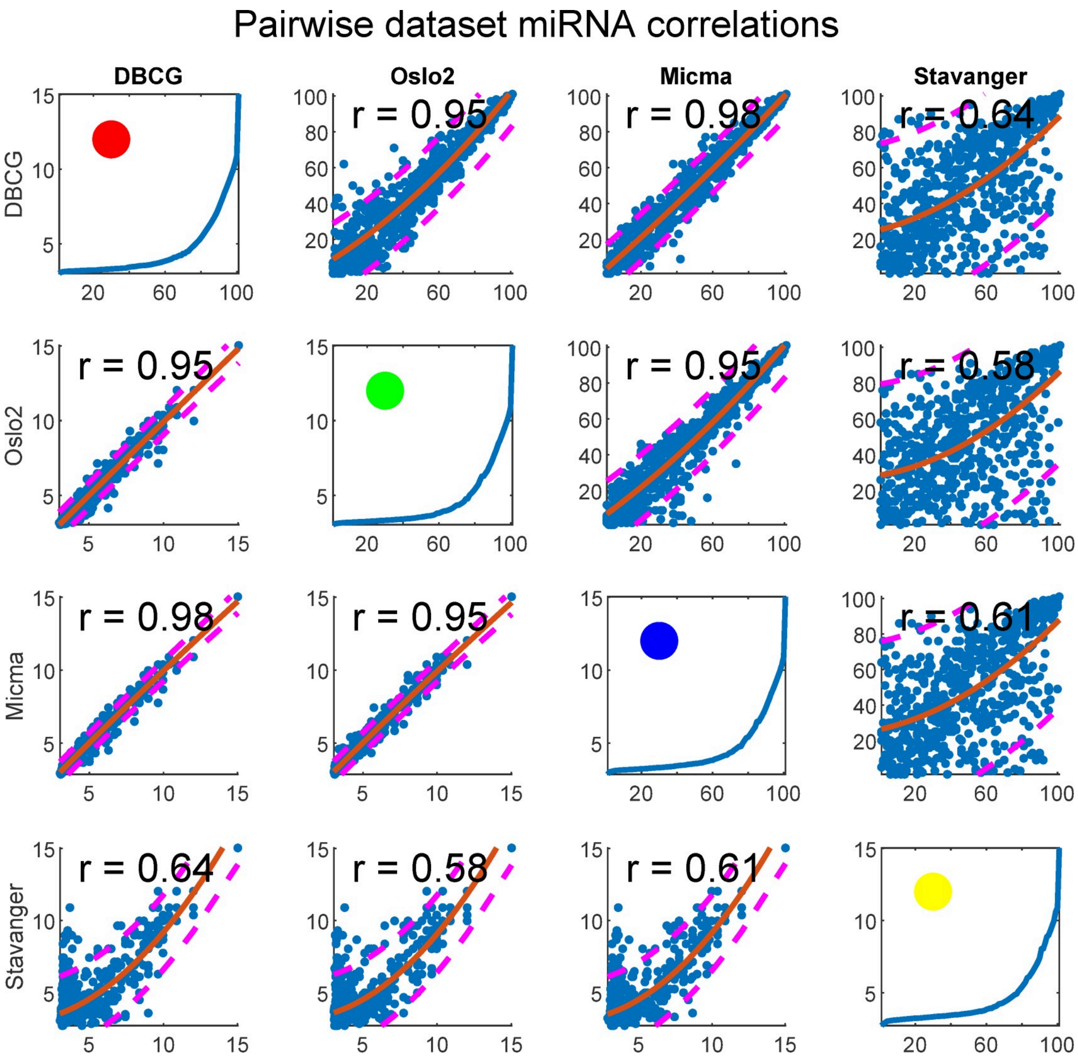

Fig 13. Scatterplot matrix of quantile normalized data showing miRNA expression reproducibility across dataset pairs. Each subplot depicts a pair of datasets. In the upper-diagonal-subplots, each point corresponds to a single miRNA's median (across samples) rank (intra-sample) in each dataset. Similarly, the bottom-diagonal shows median log2 expressions in place of ranks. A second degree polynomial curve is fitted and prediction intervals at confidence level 0.8 are plotted as dashed lines. Spearman correlation is given for each subplot. Figures at the diagonal show percentile plotted against expression and a circle represents the dataset colorcode as related to other figures in the paper.

https://doi.org/10.1371/journal.pcbi.1008608.g013

behave differently, presumably due to its fundamentally different measurement technology (Exiqon LNA—Locked Nucleic Acids vs Agilent Microarray).

We further visualize the batch-clustering behavior of the unnormalized joint dataset in Fig 14. On the left panel (A) we present hierarchical clustering of the data. Edges of sub-trees in the dendrogram are color-coded by the dataset when all leaves in the subtree belong to samples from the same original dataset. We observe a visual clustering of colors, especially evident for yellow (Stavanger) being clustered as an outgroup. In the middle panel (B) we show a silhouette plot, depicting the clustering consistency according to dataset. We observe a substantial portion of samples that are well assigned to their cluster with large silhouette values, and only a small portion are mis-assigned, again showcasing how batch effects dominate sample pairwise-distance pattern behavior. Finally, on the right panel (C) we present a visualization of the

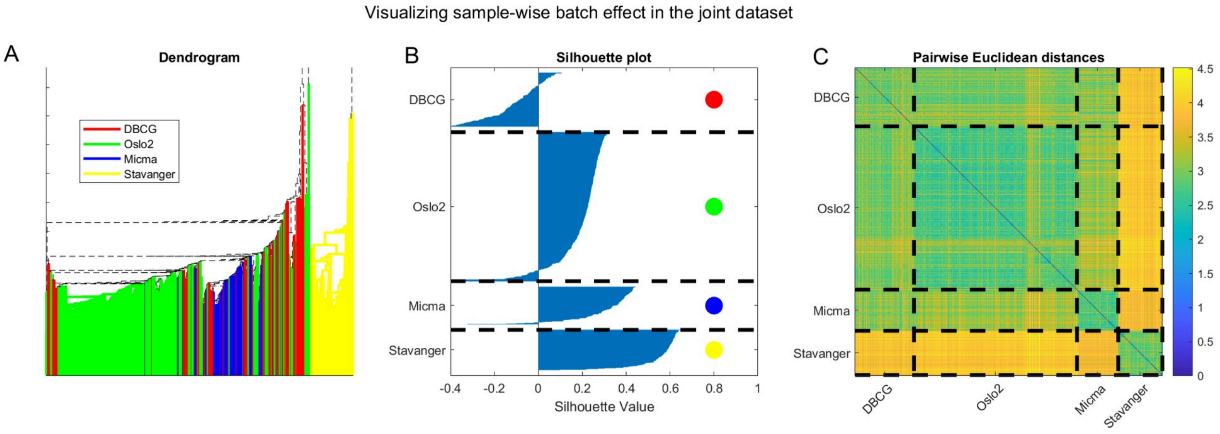

Fig 14. Visualizing batch effects in the combined cross-tech miRNA dataset considering the unnormalized data. (A) Dendrogram with edges colored by dataset. Note that the tree root is outside the displayed axis range. (B) Silhouette plot [67] showing that most samples cluster according to the dataset they originate from. (C) Pairwise Euclidean distances showing a block structure that agrees with the sample dataset of origin.

https://doi.org/10.1371/journal.pcbi.1008608.g014

sample-wise pairwise Euclidean distance matrix with dashed lines separating between samples of the same dataset. The block-diagonal structure that evidently results from coloring according to distances corresponds well to the dashed lines separating samples from different datasets. This analysis demonstrates the prevalence of batch effects in the joint datasets.

Adjusted quantile normalization (AQuN)

In this section we describe our quantile-normalization-based strategy for analyzing combined cross-technology miRNA datasets.

Let *M* be a batch collected, joint dataset. $M \in R^{n \times m}$ where *M*(*i*,*j*) is the log measured intensity value of miRNA *i* in sample *j*. We note that the *j*-th column of *M*, denoted *M*(:,*j*), corresponds to the *j*-th sample and that the *i*-th row, *M*(*i*,:) corresponds to the *i*-th miRNA in the joint dataset.

Define *β*(*M*(:,*j*)) = *k* as the experiment batch id during which sample *j* was collected.

We note the following distinction between missing values in *M*:

$$M(i,j) = \begin{cases} nan & miRNA\ i\ was\ not\ sampled\ in\ \beta(M(:,j)) \\ 0 & miRNA\ i\ was\ sampled\ in\ \beta(M(:,j))\ but\ not\ detected\ in\ sample\ j \\ \geq 0 & otherwise \end{cases}$$

Let *MFP*(*i*,*j*) = 1 if miRNA *i* is missing from platform *β*(*M*(:,*j*)) and *MFP*(*i*,*j*) = 0 otherwise (indicates if *i* is missing in the platform *j* was measured in).

	Adjusted Quantile Normalization (*M*):	
1.	$\mathcal{D} \leftarrow M + N(0, \epsilon)$	Jitter *M* to break rank ties.
2.	Let *P*(*i*,*j*) = the percentile of $\mathcal{D}(i,j)$ within $\mathcal{D}(:,j)$.	*nan*s are ignored in percentile computation. Note: *P*(*i*,*j*)∈ [0,100]
3.	$Q(i,j) = \underset{1 \leq t \leq m}{median} \{\mathcal{D}(s,t) : P(s,t) = p(i,j)\}$	Transforms values to the cross-sample-median of the corresponding per-sample-quantile.
4.	*Q*(*i*,*j*) = *nan* if *MFP*(*i*,*j*) = 1	

https://doi.org/10.1371/journal.pcbi.1008608.t004

A description of this process in words is that it replaces all present expression values with the corresponding median value of all samples within the same percentile. The underlying assumption is that a measured expression is volatile due to technical differences and measurement noise, however, (sample-based) percentiles are assumed to be stable up to the biological differences between samples. In addition—platform coverage differences are addressed.

The overall impact of applying AQuN to the distribution of expression values and to quantified batch effects as measured by the silhouette coefficient is further presented in S1 Fig.

Functional experiments

Functional experiments were performed as previously described [32, 33] with the breast cancer cell lines MCF7 and KPL-4. The lysate microarray data measuring apoptosis in the form of cleaved PARP (cPARP), HER2 and phosphorylated ERK (pERK) protein levels after 72 hours were previously published (data taken from S2 Table of referenced paper and provided as S7 Table herein) [32]. Values ±2 × standard deviation (SD) were considered as significant, which corresponded to a threshold of |1.96|. For the cell viability data, MCF7 cells were transfected with the Dharmacon miRIDIAN microRNA mimic library v.10.1 (20 nM) and incubated for 72 hours. The cell viability was measured with CellTiter-Glo assay (Promega Corp, Madison, WI, USA) according to manufacturer's protocol. The experiments were done with two biological replicates. The data were normalized by a Loess method [64] and log2-transformed. Values ±2 × SD, were considered as significant, which corresponded to a threshold of |0.2|. In both experiments the average of two different miRNA mimic controls from two replicates was used as negative controls (miRIDIAN microRNA Mimic Negative Control #1 from Dharmacon and pre-miR negative control #2 from Ambion). The transfection efficiency of miRNA mimics has been determined previously [33].

MiTEA algorithm overview

Briefly, for each prefix $\Pi_{\mathrm{B}}(\mathcal{C}_v)$ of B most-prominent candidate targets in $\mathcal{C}_v$, MiTEA produces a binary vector, $\mathcal{B}(\mu, v, B)$, such that, g_i, the i-th gene in $\mathcal{G}_\mu$ is labeled "1" if and only if it is in the candidate prefix, i.e. $g_i \in \Pi_{\mathrm{B}}(\mathcal{C}_v)$. MiTEA then computes an approximate minimum hypergeometric (mHG [36, 57]) P-value to quantify whether the B proposed targets are enriched at the top of the $\mathcal{G}_\mu$ list or not. Finally–MITEA applies an FDR correction (using the Benjamini-Hochberg procedure [65]) across evaluated vs and reports the set of miRNAs associated with the ranked target list $\mathcal{G}_\mu$ and their associated Q-values.

Supporting information

S1 Data. A zip file containing figures for the top 40 differentially expressed miRNA (post-normalization) on ER clinical label. Contains additional figures per miRNA pertaining to the analysis presented in Fig 2.
(ZIP)

S2 Data. A zip file containing quality control reports for miRNA datasets. Generated by the arrayQualityMetrics package, as described in "Dataset pre-processing and coverage". Open index.html in either folder to view the detailed report data.
(ZIP)

S3 Data. A zip file containing quality control reports for mRNA datasets. Generated by the arrayQualityMetrics package, as described in "Dataset pre-processing and coverage". Open

index.html in either folder to view the detailed report data.
(ZIP)

S1 Fig. Top) Kernel density estimates of each sample colored by their corresponding dataset. The resulting normalized distribution is overlaid in black. Bottom) Impact of normalization on per-sample silhouette coefficient measured for clustering by dataset. 602/745 samples have lower silhouette coefficients after normalization in comparison to before normalization, demonstrating an overall alleviation of batch effect per dataset. Marginal distributions are shown to highlight differences between datasets.
(TIF)

S2 Fig. Venn diagram comparing the number of differentially expressed miRNAs surfaced by different normalization approaches. We observe a larger set of unique miRNAs detected by our normalization approach compared to other approaches.
(TIF)

S3 Fig. Histograms of Sample-wise and miRNA-wise Spearman correlation coefficient (ρ) between expression before and after normalization.
(TIF)

S4 Fig. Differential expression analysis on TCGA, Tahiri cohorts (Cancer vs. Normal tissue). The results shown here follow the same analysis described in Fig 3 in the manuscript. We note the additional evaluated method "Percentile Normalization" was added as it is only relevant in a case-vs-control setup, as evaluated here. Note that the "Percentile Normalization" curve is overlaid by the random permutation curves (dashed black curves).
(TIF)

S1 Table. A set of known oncomirs (Wikipedia) their Q-value (cells conditionally formatted from green to red) and ranks (cells conditionally formatted from blue to red) when sorted according to the differential expression Q-value from the analysis shown in S4 Fig. We observe a higher set of oncomirs return as differentially expressed, and many are more highly ranked (including very prominent ones such as miR-21, miR-18a).
(XLSX)

S2 Table. An extension of the analysis presented in Table 2 which includes a comparison with an additional normalization method (Vanilla quantile) and across two more datasets (Micma and Stavanger).
(XLSX)

S3 Table. Joint dataset table raw measurement data as depicted in Fig 12.
(XLSX)

S4 Table. Joint dataset table from S3 Table, normalized by AQuN.
(XLSX)

S5 Table. Corresponding clinical labels for S3 Table and S4 Table.
(XLSX)

S6 Table. A list of 33 unique differentially expressed miRNAs between ER positive vs ER negative as identified by our normalization method.
(XLSX)

S7 Table. Functional experiment results table presented as S2 Table published in Leivonen S-K et al. [32].
(XLSX)

S1 Text. Discussion on joint one-color and two-color analysis of available Stavanger data.
(DOCX)

S2 Text. Caption for S2 Fig–Venn diagram of differential expression results.
(DOCX)

S3 Text. Caption for S3 Fig and discussion on AQuN impact on data rankings.
(DOCX)

Acknowledgments

We thank the Yakhini research group for important insights and comments throughout the research process. We thank Prof. Benny Chor for his advice and encouragement for pursuing this work.

The results published here are in whole or part based upon data generated by the TCGA Research Network: https://www.cancer.gov/tcga.

MR Aure was a postdoctoral fellow of the South Eastern Norway Health Authority (https://www.helse-sorost.no/south-eastern-norway-regional-health-authority) under grant 2014021 to Anne-Lise Børresen-Dale and a research fellow of the Norwegian Cancer Society (https://kreftforeningen.no/en/about-us/) under grant 711164 to Vessela N Kristensen.

The Stavanger database was sponsored by grants from the Folke Hermansen Foundation in 2007, a grant provided by the Stavanger University Hospital research fund in 2009 and a PhD-fellowship from Helse Vest in 2009.

Folke Hermansen Foundation (http://www.folke-fondet.org/) grant 2007 entitled "Early breast cancer prognostication by genomics and proteomics", EAMJ received the unnumbered grant.

Stavanger University Hospital, research department (https://helse-stavanger.no/en) grant entitled “Comparing the prognostic and predictive value of microRNA, gene expression signatures and proliferation in early node negative breast cancer”, EAMJ received the unnumbered grant.

Author Contributions

Conceptualization: Shay Ben-Elazar, Miriam Ragle Aure, Suvi-Katri Leivonen, Ole Christian Lingjærde.

Data curation: Miriam Ragle Aure, Kristin Jonsdottir, Suvi-Katri Leivonen, Kristine Kleivi Sahlberg.

Formal analysis: Shay Ben-Elazar, Miriam Ragle Aure, Zohar Yakhini.

Funding acquisition: Miriam Ragle Aure, Vessela N. Kristensen, Emiel A. M. Janssen, Zohar Yakhini.

Investigation: Shay Ben-Elazar, Miriam Ragle Aure, Kristin Jonsdottir, Suvi-Katri Leivonen, Kristine Kleivi Sahlberg, Zohar Yakhini.

Methodology: Shay Ben-Elazar, Miriam Ragle Aure, Ole Christian Lingjærde, Zohar Yakhini.

Project administration: Shay Ben-Elazar, Zohar Yakhini.

Resources: Vessela N. Kristensen, Emiel A. M. Janssen, Kristine Kleivi Sahlberg, Zohar Yakhini.

Software: Shay Ben-Elazar.

Supervision: Vessela N. Kristensen, Emiel A. M. Janssen, Kristine Kleivi Sahlberg, Ole Christian Lingjærde, Zohar Yakhini.

Validation: Shay Ben-Elazar, Miriam Ragle Aure, Suvi-Katri Leivonen, Zohar Yakhini.

Visualization: Shay Ben-Elazar.

Writing – original draft: Shay Ben-Elazar, Miriam Ragle Aure, Zohar Yakhini.

Writing – review & editing: Shay Ben-Elazar, Miriam Ragle Aure, Kristin Jonsdottir, Suvi-Katri Leivonen, Vessela N. Kristensen, Emiel A. M. Janssen, Kristine Kleivi Sahlberg, Ole Christian Lingjærde, Zohar Yakhini.

References

1. Bartel DP. MicroRNAs:Target Recognition and Regulatory Functions. Cell. 2009; 136:215–233. https://doi.org/10.1016/j.cell.2009.01.002 PMID: 19167326
2. Chen Y, Stallings RL. Differential Patterns of MicroRNA Expression in Neuroblastoma Are Correlated with Prognosis, Differentiation, and Apoptosis. Cancer Res. 2007; 67:976–983. https://doi.org/10.1158/0008-5472.CAN-06-3667 PMID: 17283129
3. Tricoli J V., Jacobson JW. MicroRNA:Potential for Cancer Detection, Diagnosis, and Prognosis. Cancer Res. 2007; 67:4553–4555. https://doi.org/10.1158/0008-5472.CAN-07-0563 PMID: 17510380
4. Schepeler T, Reinert JT, Ostenfeld MS, Christensen LL, Silahtaroglu AN, Dyrskjot L, et al. Diagnostic and Prognostic MicroRNAs in Stage II Colon Cancer. Cancer Res. 2008; 68:6416–6424. https://doi.org/10.1158/0008-5472.CAN-07-6110 PMID: 18676867
5. Aure MR, Vitelli V, Jernström S, Kumar S, Krohn M, Due EU, et al. Integrative clustering reveals a novel split in the luminal A subtype of breast cancer with impact on outcome. Breast Cancer Res. 2017; 19:44. https://doi.org/10.1186/s13058-017-0812-y PMID: 28356166
6. Cancer Genome Atlas Network. Comprehensive molecular portraits of human breast tumours. Nature. 2012; 490:61–70. https://doi.org/10.1038/nature11412 PMID: 23000897
7. Dvinge H, Git A, Gräf S, Salmon-Divon M, Curtis C, Sottoriva A, et al. The shaping and functional consequences of the microRNA landscape in breast cancer. Nature. 2013; 497:378–382. https://doi.org/10.1038/nature12108 PMID: 23644459
8. Navon R, Wang H, Steinfeld I, Tsalenko A, Ben-Dor A, Yakhini Z. Novel Rank-Based Statistical Methods Reveal MicroRNAs with Differential Expression in Multiple Cancer Types. Preiss T, editor. PLoS One. 2009; 4:e8003. https://doi.org/10.1371/journal.pone.0008003 PMID: 19946373
9. Cohn-Alperovich D, Rabner A, Kifer I, Mandel-Gutfreund Y, Yakhini Z. Mutual enrichment in aggregated ranked lists with applications to gene expression regulation. Bioinformatics. 2016; 32:i464–i472. https://doi.org/10.1093/bioinformatics/btw435 PMID: 27587663
10. Aure MR, Jernström S, Krohn M, Vollan HKM, Due EU, Rødland E, et al. Integrated analysis reveals microRNA networks coordinately expressed with key proteins in breast cancer. Genome Med. 2015; 7:21. https://doi.org/10.1186/s13073-015-0135-5 PMID: 25873999
11. Enerly E, Steinfeld I, Kleivi K, Leivonen S-K, Aure MR, Russnes HG, et al. miRNA-mRNA Integrated Analysis Reveals Roles for miRNAs in Primary Breast Tumors. Creighton C, editor. PLoS One. 2011; 6:e16915. https://doi.org/10.1371/journal.pone.0016915 PMID: 21364938
12. Lesurf R, Aure MR, Mørk HH, Vitelli V, Lundgren S, Børresen-Dale A-L, et al. Molecular Features of Subtype-Specific Progression from Ductal Carcinoma In Situ to Invasive Breast Cancer. Cell Rep. 2016; 16:1166–1179. https://doi.org/10.1016/j.celrep.2016.06.051 PMID: 27396337
13. Haakensen VD, Nygaard V, Greger L, Aure MR, Fromm B, Bukholm IRK, et al. Subtype-specific microRNA expression signatures in breast cancer progression. Int J Cancer. 2016; 139:1117–1128. https://doi.org/10.1002/ijc.30142 PMID: 27082076
14. Tahiri A, Leivonen S-K, Lüders T, Steinfeld I, Ragle Aure M, Geisler J, et al. Deregulation of cancer-related miRNAs is a common event in both benign and malignant human breast tumors. Carcinogenesis. 2014; 35:76–85. https://doi.org/10.1093/carcin/bgt333 PMID: 24104550

15. Wang M, Xu S. Statistical power in genome-wide association studies and quantitative trait locus mapping. Heredity (Edinb). 2019; 123:287–306. https://doi.org/10.1038/s41437-019-0205-3 PMID: 30858595

16. Hong EP, Park JW. Sample size and statistical power calculation in genetic association studies. Genomics Inform. 2012; 10:117–22. https://doi.org/10.5808/GI.2012.10.2.117 PMID: 23105939

17. Git A, Dvinge H, Salmon-Divon M, Osborne M, Kutter C, Hadfield J, et al. Systematic comparison of microarray profiling, real-time PCR, and next-generation sequencing technologies for measuring differential microRNA expression. RNA. 2010; 16:991–1006. https://doi.org/10.1261/rna.1947110 PMID: 20360395

18. Mestdagh P, Hartmann N, Baeriswyl L, Andreasen D, Bernard N, Chen C, et al. Evaluation of quantitative miRNA expression platforms in the microRNA quality control (miRQC) study. Nat Methods. 2014; 11:809–815. https://doi.org/10.1038/nmeth.3014 PMID: 24973947

19. Nygaard V, Rødland EA, Hovig E. Methods that remove batch effects while retaining group differences may lead to exaggerated confidence in downstream analyses. Biostatistics. 2016; 17:29–39. https://doi.org/10.1093/biostatistics/kxv027 PMID: 26272994

20. Sims AH, Smethurst GJ, Hey Y, Okoniewski MJ, Pepper SD, Howell A, et al. The removal of multiplicative, systematic bias allows integration of breast cancer gene expression datasets—improving meta-analysis and prediction of prognosis. BMC Med Genomics. 2008; 1:42. https://doi.org/10.1186/1755-8794-1-42 PMID: 18803878

21. Gibbons SM, Duvallet C, Alm EJ. Correcting for batch effects in case-control microbiome studies. Langille M, editor. PLoS Comput Biol. 2018; 14:e1006102. https://doi.org/10.1371/journal.pcbi.1006102 PMID: 29684016

22. Hulin J-A, Tommasi S, Elliot D, Hu DG, Lewis BC, Mangoni AA. MiR-193b regulates breast cancer cell migration and vasculogenic mimicry by targeting dimethylarginine dimethylaminohydrolase 1. Sci Rep. 2017; 7:13996. https://doi.org/10.1038/s41598-017-14454-1 PMID: 29070803

23. Hashemi ZS, Forouzandeh Moghadam M, Khalili S, Ghavami M, Salimi F, Sadroddiny E. Additive effect of metastamiR-193b and breast cancer metastasis suppressor 1 as an anti-metastatic strategy. Breast Cancer. 2019; 26:215–228. https://doi.org/10.1007/s12282-018-0915-z PMID: 30284194

24. Myhre S, Mohammed H, Tramm T, Alsner J, Finak G, Park M, et al. In Silico Ascription of Gene Expression Differences to Tumor and Stromal Cells in a Model to Study Impact on Breast Cancer Outcome. Algül H, editor. PLoS One. 2010; 5:e14002. https://doi.org/10.1371/journal.pone.0014002 PMID: 21124964

25. Tramm T, Mohammed H, Myhre S, Kyndi M, Alsner J, Borresen-Dale A-L, et al. Development and Validation of a Gene Profile Predicting Benefit of Postmastectomy Radiotherapy in Patients with High-Risk Breast Cancer:A Study of Gene Expression in the DBCG82bc Cohort. Clin Cancer Res. 2014; 20:5272–5280. https://doi.org/10.1158/1078-0432.CCR-14-0458 PMID: 25149560

26. Janssen EAM, Slewa A, Gudlaugsson E, Jonsdottir K, Skaland I, Søiland H, et al. Biologic profiling of lymph node negative breast cancers by means of microRNA expression. Mod Pathol. 2010; 23:1567–1576. https://doi.org/10.1038/modpathol.2010.177 PMID: 20818337

27. Amaratunga D, Cabrera J. Analysis of Data From Viral DNA Microchips. J Am Stat Assoc. 2001; 96:1161–1170. https://doi.org/10.1198/016214501753381814

28. Johnson WE, Li C, Rabinovic A. Adjusting batch effects in microarray expression data using empirical Bayes methods. Biostatistics. 2007; 8:118–127. https://doi.org/10.1093/biostatistics/kxj037 PMID: 16632515

29. J M. Extract linearly independent subset of matrix columns—File Exchange—MATLAB Central. MATLAB Central File Exchange; 2020. Available from: https://www.mathworks.com/matlabcentral/fileexchange/77437-extract-linearly-independent-subset-of-matrix-columns

30. Cizeron-Clairac G, Lallemand F, Vacher S, Lidereau R, Bieche I, Callens C. MiR-190b, the highest up-regulated miRNA in ERα-positive compared to ERα-negative breast tumors, a new biomarker in breast cancers? BMC Cancer. 2015; 15:499. https://doi.org/10.1186/s12885-015-1505-5 PMID: 26141719

31. Zhou L, Li Z, Pan X, Lai Y, Quan J, Zhao L, et al. Identification of miR-18a-5p as an oncogene and prognostic biomarker in RCC. Am J Transl Res. 2018; 10:1874. Available from: https://www.ncbi.nlm.nih.gov/pmc/articles/PMC6038077/ PMID: 30018727

32. Leivonen S-K, Sahlberg KK, Mäkelä R, Due EU, Kallioniemi O, Børresen-Dale A-L, et al. High-throughput screens identify microRNAs essential for HER2 positive breast cancer cell growth. Mol Oncol. 2014; 8:93–104. https://doi.org/10.1016/j.molonc.2013.10.001 PMID: 24148764

33. Leivonen S-K, Mäkelä R, Ostling P, Kohonen P, Haapa-Paananen S, Kleivi K, et al. Protein lysate microarray analysis to identify microRNAs regulating estrogen receptor signaling in breast cancer cell lines. Oncogene. 2009; 28:3926–36. https://doi.org/10.1038/onc.2009.241 PMID: 19684618

34. Hu J-Y, Yi W, Wei X, Zhang M-Y, Xu R, Zeng L-S, et al. miR-601 is a prognostic marker and suppresses cell growth and invasion by targeting PTP4A1 in breast cancer. Biomed Pharmacother. 2016; 79:247–53. https://doi.org/10.1016/j.biopha.2016.02.014 PMID: 27044835

35. Li C, Yu S, Wu S, Ni Y, Pan Z. MicroRNA-936 targets FGF2 to inhibit epithelial ovarian cancer aggressiveness by deactivating the PI3K/Akt pathway. Onco Targets Ther. 2019; 12:5311–5322. https://doi.org/10.2147/OTT.S213231 PMID: 31371979

36. Eden E, Navon R, Steinfeld I, Lipson D, Yakhini Z. GOrilla:a tool for discovery and visualization of enriched GO terms in ranked gene lists. BMC Bioinformatics. 2009; 10:48. https://doi.org/10.1186/1471-2105-10-48 PMID: 19192299

37. Steinfeld I, Navon R, Ach R, Yakhini Z. miRNA target enrichment analysis reveals directly active miRNAs in health and disease. Nucleic Acids Res. 2013; 41:e45–e45. https://doi.org/10.1093/nar/gks1142 PMID: 23209027

38. Agarwal V, Bell GW, Nam J-W, Bartel DP. Predicting effective microRNA target sites in mammalian mRNAs. Elife. 2015; 4. https://doi.org/10.7554/eLife.05005 PMID: 26267216

39. Kwon JJ, Factora TD, Dey S, Kota J. A Systematic Review of miR-29 in Cancer. Mol Ther oncolytics. 2019; 12:173–194. https://doi.org/10.1016/j.omto.2018.12.011 PMID: 30788428

40. Wang C, Bian Z, Wei D, Zhang J. miR-29b regulates migration of human breast cancer cells. Mol Cell Biochem. 2011; 352:197–207. https://doi.org/10.1007/s11010-011-0755-z PMID: 21359530

41. Shinden Y, Iguchi T, Akiyoshi S, Ueo H, Ueda M, Hirata H, et al. miR-29b is an indicator of prognosis in breast cancer patients. Mol Clin Oncol. 2015; 3:919–923. https://doi.org/10.3892/mco.2015.565 PMID: 26171207

42. Ni X, Xia T, Zhao Y, Zhou W, Wu N, Liu X, et al. Downregulation of miR-106b induced breast cancer cell invasion and motility in association with overexpression of matrix metalloproteinase 2. Cancer Sci. 2014; 105:18–25. https://doi.org/10.1111/cas.12309 PMID: 24164962

43. Lee J, Kim HE, Song Y-S, Cho EY, Lee A. miR-106b-5p and miR-17-5p could predict recurrence and progression in breast ductal carcinoma in situ based on the transforming growth factor-beta pathway. Breast Cancer Res Treat. 2019; 176:119–130. https://doi.org/10.1007/s10549-019-05192-1 PMID: 30989460

44. Zheng R, Pan L, Gao J, Ye X, Chen L, Zhang X, et al. Prognostic value of miR-106b expression in breast cancer patients. J Surg Res. 2015; 195:158–165. https://doi.org/10.1016/j.jss.2014.12.035 PMID: 25619461

45. Ye F, Tang H, Liu Q, Xie X, Wu M, Liu X, et al. miR-200b as a prognostic factor in breast cancer targets multiple members of RAB family. J Transl Med. 2014; 12:17. https://doi.org/10.1186/1479-5876-12-17 PMID: 24447584

46. Yao Y, Hu J, Shen Z, Yao R, Liu S, Li Y, et al. MiR-200b expression in breast cancer:a prognostic marker and act on cell proliferation and apoptosis by targeting Sp1. J Cell Mol Med. 2015; 19:760–769. https://doi.org/10.1111/jcmm.12432 PMID: 25639535

47. Zheng Q, Cui X, Zhang D, Yang Y, Yan X, Liu M, et al. miR-200b inhibits proliferation and metastasis of breast cancer by targeting fucosyltransferase IV and α1,3-fucosylated glycans. Oncogenesis. 2017; 6: e358–e358. https://doi.org/10.1038/oncsis.2017.58 PMID: 28692034

48. Zhang L. The role of microRNA, mir-30d, in the initiation and progression of cancer. [cited 16 Oct 2019]. Available from: http://grantome.com/grant/NIH/R01-CA142776-05

49. Yang S-J, Yang S-Y, Wang D-D, Chen X, Shen H-Y, Zhang X-H, et al. The miR-30 family:Versatile players in breast cancer. Tumor Biol. 2017; 39:101042831769220. https://doi.org/10.1177/1010428317692204 PMID: 28347244

50. Hong Y, Liang H, Uzair-ur-Rehman, Wang Y, Zhang W, Zhou Y, et al. miR-96 promotes cell proliferation, migration and invasion by targeting PTPN9 in breast cancer. Sci Rep. 2016; 6:37421. https://doi.org/10.1038/srep37421 PMID: 27857177

51. Xie W, Sun F, Chen L, Cao X. miR-96 promotes breast cancer metastasis by suppressing MTSS1. Oncol Lett. 2018; 15:3464–3471. https://doi.org/10.3892/ol.2018.7728 PMID: 29456723

52. Zhang X, Ma G, Liu J, Zhang Y. MicroRNA-182 promotes proliferation and metastasis by targeting FOXF2 in triple-negative breast cancer. Oncol Lett. 2017; 14:4805–4811. https://doi.org/10.3892/ol.2017.6778 PMID: 29085483

53. Chiang C-H, Hou M-F, Hung W-C. Up-regulation of miR-182 by β-catenin in breast cancer increases tumorigenicity and invasiveness by targeting the matrix metalloproteinase inhibitor RECK. Biochim Biophys Acta—Gen Subj. 2013; 1830:3067–3076. https://doi.org/10.1016/j.bbagen.2013.01.009 PMID: 23333633

54. Luna C, Li G, Qiu J, Epstein DL, Gonzalez P. Role of miR-29b on the regulation of the extracellular matrix in human trabecular meshwork cells under chronic oxidative stress. Mol Vis. 2009; 15:2488–97. Available from: http://www.ncbi.nlm.nih.gov/pubmed/19956414 PMID: 19956414

55. Liu Y, Zhang J, Sun X, Su Q, You C. Down-regulation of miR-29b in carcinoma associated fibroblasts promotes cell growth and metastasis of breast cancer. Oncotarget. 2017; 8:39559. https://doi.org/10.18632/oncotarget.17136 PMID: 28465475

56. Faul F, Erdfelder E, Lang A-G, Buchner A. G*Power 3:a flexible statistical power analysis program for the social, behavioral, and biomedical sciences. Behav Res Methods. 2007; 39:175–91. Available from: http://www.ncbi.nlm.nih.gov/pubmed/17695343 https://doi.org/10.3758/bf03193146 PMID: 17695343

57. Eden E, Lipson D, Yogev S, Yakhini Z. Discovering motifs in ranked lists of DNA sequences. PLoS Comput Biol. 2007; 3:0508–0522. https://doi.org/10.1371/journal.pcbi.0030039 PMID: 17381235

58. Lingle W, Erickson BJ, Zuley ML, Jarosz R, Bonaccio E, Filippini J, et al. Radiology Data from The Cancer Genome Atlas Breast Invasive Carcinoma [TCGA-BRCA] collection. The Cancer Imaging Archive; 2016. https://doi.org/10.7937/K9/TCIA.2016.AB2NAZRP

59. Oncomir—Wikipedia. [cited 7 Nov 2020]. Available from: https://en.wikipedia.org/wiki/Oncomir#List_of_identified_oncomirs

60. Ritchie ME, Phipson B, Wu D, Hu Y, Law CW, Shi W, et al. limma powers differential expression analyses for RNA-sequencing and microarray studies. Nucleic Acids Res. 2015; 43:e47–e47. https://doi.org/10.1093/nar/gkv007 PMID: 25605792

61. Ritchie ME, Silver J, Oshlack A, Holmes M, Diyagama D, Holloway A, et al. A comparison of background correction methods for two-colour microarrays. Bioinformatics. 2007; 23:2700–2707. https://doi.org/10.1093/bioinformatics/btm412 PMID: 17720982

62. Xu T, Su N, Liu L, Zhang J, Wang H, Zhang W, et al. miRBaseConverter:An R/Bioconductor Package for Converting and Retrieving miRNA Name, Accession, Sequence and Family Information in Different Versions of miRBase. bioRxiv. 2018; 407148. https://doi.org/10.1101/407148

63. Kauffmann A, Gentleman R, Huber W. arrayQualityMetrics—a bioconductor package for quality assessment of microarray data. Bioinformatics. 2009; 25:415–416. https://doi.org/10.1093/bioinformatics/btn647 PMID: 19106121

64. Boutros M, Brás LP, Huber W. Analysis of cell-based RNAi screens. Genome Biol. 2006; 7:R66. https://doi.org/10.1186/gb-2006-7-7-R66 PMID: 16869968

65. Benjamini Y, Hochberg Y. Controlling the False Discovery Rate:A Practical and Powerful Approach to Multiple Testing. J R Stat Soc Ser B. 1995; 57:289–300. https://doi.org/10.1111/j.2517-6161.1995.tb02031.x

66. Cohen J. Statistical power analysis for the behavioral sciences. Academic Press; 1977.

67. Rousseeuw PJ. Silhouettes:A graphical aid to the interpretation and validation of cluster analysis. J Comput Appl Math. 1987; 20:53–65. https://doi.org/10.1016/0377-0427(87)90125-7